USER SELECTION WITH PERFECT AND NO PRIMARY CSIT IN MIMO COGNITIVE RADIO NETWORKS

A Dissertation by

Wenhao Xiong

Master of Science, Wichita State University, 2009

Bachelor of Science, University of Electric of Science and Technology of China, 2007

Submitted to the Department of Electrical Engineering and Computer Science
and the faculty of the Graduate School of
Wichita State University
in partial fulfillment of
the requirements for the degree of
Doctor of Philosophy

December 2014

USER SELECTION WITH PERFECT AND NO PRIMARY CSIT IN MIMO COGNITIVE RADIO NETWORKS

The following faculty members have examined the final copy of this dissertation for form and content, and recommend that it be accepted in partial fulfillment of the requirement for the degree of Doctor of Philosophy with a major in Electrical Engineering.

_____
Hyuck M. Kwon, Committee Chair

_____
John Watkins, Committee Member

_____
Mahmoud E. Sawan, Committee Member

_____
Visvakumar Aravinthan, Committee Member

_____
Xiaomi Hu, Committee Member

Accepted for the College of Engineering

_____
Royce Bowden, Dean

Accepted for the Graduate School

_____
Abu S.M. Masud, Interim Dean

DEDICATION

To my parents and my girlfriend

ACKNOWLEDGEMENTS

I would like to thank my advisor, Dr. Hyuck M. Kwon, who made it possible for me to complete this dissertation. His support, knowledge, and patience have guided me from the very beginning to the end. I would also like to thank Dr. John Watkins, Dr. Mahmoud E. Sawan, Dr. Visvakumar Aravinthan, and Dr. Xiaomi Hu for their kind help and for serving on my dissertation committee. Last, but not the least, I want to thank my parents Kaike Xiong and Yuan Yuan and my girlfriend Da Ma for their continuous support and encouragement.

ABSTRACT

Spectrum is one of the most precious resources in the field of wireless communication field. As the number of users and demand for fast data transmission increases, the current spectrum resources become insufficient. Cognitive radio (CR) networks are one of the promising ways to increase the efficiency of spectrum use. While a licensed primary user (PU) occupies a certain bandwidth, CR users try to utilize the same bandwidth under the condition that interference is minimized and the licensed user is able to achieve its required data rate. It is desirable to allow as many CR users into the bandwidth as possible, thus maximizing spectrum efficiency. However, with a large number of secondary users (SUs), interference becomes significant. Hence, only a portion of the CR users can be served in most cases. This work involves the study of user selection (US) strategies for a multiple-input multiple-output (MIMO) CR downlink network, where the r-antenna underlay CR SUs coexist with the PU, and all terminals are equipped with multiple antennas. Two main scenarios are considered: (1) the t-antenna cognitive base station (CBS) has perfect or partial channel state information at the transmitter (CSIT) from the CBS to the PU receiver (RX), and (2) the CBS has absolutely no PU CSIT. For these scenarios, multiple SU selection schemes that are applicable to both best-effort PU interference mitigation and hard interference temperature constraints are proposed and evaluated. Also, in this dissertation scheduling methods for non-orthogonal resource sharing between device-to-device (D2D) and cellular-user equipment (C-UE) in a multi-carrier multi-antenna network are examined. The cellular eNodeB (eNB) allocates a pool of subchannels that may be used autonomously by D2D user equipment (UE) for D2D discovery and communication. Then, the scheduling of C-UE uplink transmissions in the same subchannel pool based on a best-effort C-UE-to-D2D interference mitigation method that does not require knowledge of C-UE to D2D UE channels is proposed. The selection criterion is a combination of the number of spatial streams, subchannels, and transmit power needed by C-UE to achieve their target data rate.

TABLE OF CONTENTS

Chapter **Page**

LIST OF FIGURES

Figure **Page**

LIST OF ABBREVIATIONS

AWGN	Additive White Gaussian Noise
BD	Block Diagonalization
BWF	Balanced Water-Filling
CBS	Cognitive Base Station
CDMA	Code Division Multiple Access
CSI	Channel State Information
CSIT	Channel State Information at the Transmitter
CSUS	Channel Similarity-based User Selection
C-UE	Cellular-User Equipment
CWF	Classical Water-Filling
DSA	Dynamic Spectrum Access
D2D	Device-to-Device
eNB	eNodeB
FWF	Frugal Water-Filling
IT	Interference Temperature
LTE	Long-Term Evolution
MIMO	Multiple-Input Multiple-Output
MISO	Multiple-Input Single-Output
OFDMA	Orthogonal Frequency Division Multiple Access
PA	Power Allocation
PGUS	Precoder-based Group User Selection
PU	Primary User

LIST OF ABBREVIATIONS (continued)

QoS	Quality of Service
RX	Receiver
SINR	Signal-to-Interference-plus-Noise Ratio
SOUS	Semi-Orthogonal User Selection
SUs	Secondary Users
SVD	Singular Value Decomposition
SWF	Spatial Water-Filling
TX	Transmitter
UE	User Equipment
UL	Uplink
US	User Selection

CHAPTER 1

INTRODUCTION

Dynamic spectrum access (DSA) is emerging as a promising solution to enable better utilization of the radio spectrum, by admitting more devices into underutilized frequency bands [1]. DSA categorizes wireless terminals as primary (licensed) users (PUs) and secondary users (SUs), where PUs have priority in accessing the shared spectrum. The *underlay* cognitive paradigm usually mandates that concurrent secondary and primary transmissions may occur only if the interference at the PUs due to SUs is below some acceptable threshold [1].

Multiple-input multiple-output (MIMO) systems have been extensively investigated in the context of underlay DSA networks, where multiple transmit antennas are used by SUs for beamforming and to control the interference to PUs [2]-[4]. In a typical MIMO broadcast channel, the number of cognitive base station (CBS) antennas is limited, and thus, user selection (US) strategies that serve a subset of the SUs at a given time are needed. Various user selection strategies for DSA networks have been investigated [5]-[11]. Resource allocation and admission control were studied for a single-antenna code division multiple access (CDMA)-based underlay interference network [5]. A multiple-input single-output (MISO) scenario with zero-forcing beamforming was considered [8], and single-antenna SUs whose channels are nearly orthogonal to the PU channel were preselected to minimize the interference to the primary user. Then, M best SUs, whose channels are mutually nearly orthogonal to each other, were scheduled from the preselected cognitive users. In the work of Islam et al. [9], the CBS had to satisfy the signal-to-interfrerence-plus-noise (SINR) constraints of the selected single-antenna SUs while protecting one PU from interference. In the work of Imran et al. [10], an opportunistic scheduling approach was adopted in conjunction with semi-orthogonal user selection as in the work of Hamdi et al.[8]. Driouch and Ajib [11] schedule single-antenna SUs over multiple bands by the multi-antenna CBS based on graph theory.

Note that previous work [5]-[11] has generally considered single-antenna SUs and has assumed some knowledge of the PU channel state information at the transmitter (CSIT). This dissertation considers a general MIMO cognitive broadcast channel where the CBS, SUs, primary transmitter, and PU are all equipped with multiple antennas; the novel scenario of completely unknown PU CSIT is also considered.

On the other hand, forthcoming fifth-generation cellular networks are expected to feature a mix of radio access technologies and denser cell deployments with the objective of maximizing spectrum reuse. One method of further increasing spectral and energy efficiencies, especially for short-range communications, is to create device-to-device (D2D) links for the direct transfer of data between UE without having to be routed through the base station or eNodeB (eNB) [12]. D2D communication can provide greater autonomy and resilience in cellular networks and, therefore, is currently being standardized in 3GPP Long-Term Evolution (LTE) Release 13 [13, 14].

A simple approach towards the coexistence of D2D and cellular UE (C-UE) is to partition the overall bandwidth into orthogonal portions and assign a dedicated resource (i.e., bandwidth) for D2D communications. This eliminates cross-system interference, but can be highly inefficient if the D2D resources are underutilized. Therefore, current interest is centered on non-orthogonal resource sharing between D2D and cellular UE that share the same frequency band. In such cases, careful interference management techniques that avoid degrading the QoS of C-UE and D2D UE are of significant interest.

Generally, previous work has focused on mitigating the interference caused by D2D transmissions to C-UE, and has assumed that C-UE has higher priority. In the work of Janis et al. [15], the transmit power of D2D links and the inter-UE distances are restricted in order to limit the interference to C-UE. Power control and sum-rate maximization have been studied for one C-UE and two types of D2D UE [16]. An information-theoretic link scheduling approach for additive white Gaussian noise (AWGN) channels was also adopted [17], where optimal sets of D2D users were formed such that each can decode successfully

while treating interference from others as noise. Note that only single-antenna devices were considered in several studies [15]-[29]. Wang and Wu [28] used an augmented bipartite graph approach to heuristically maximize the overall sum rate of C-UE and D2D UE. Energy-efficient precoding design for multi-antenna D2D UE with C-UE interference constraints has been analyzed [30]. Furthermore, this prior work generally assumes that the interfering cross-channels or interference levels between C-UE and D2D UE are known to a central scheduling entity, and the resource allocation and transmit power control for the D2D system is centralized.

In contrast, in this work, a different perspective has been adopted with regard to D2D resource allocation and interference management. A major driving force behind D2D communications is their use for proximity-based services and critical missions in law-enforcement or disaster scenarios. Therefore, it is also important to control the interference perceived by the D2D subsystem from C-UE; otherwise, the advantages of D2D traffic offloading will be lost. Additionally, resource allocation of D2D UEs may be performed autonomously in practice without complete eNB control. For example, in 3GPP LTE, it is assumed that a D2D operates in the uplink LTE spectrum (in the case of frequency division duplex) or uplink subframes of the cell providing coverage. Furthermore, the resource allocation for the D2D transmissions can be semi-autonomous or completely controlled by the LTE eNB. The case where D2D UE autonomously selects radio resources from a prespecified transmission resource pool for discovery signal transmission is known as Type 1 D2D discovery [14].

The main contributions of this dissertation include the following:

- When PU CSIT is perfectly or partially known to a CBS, two computationally efficient SU selection schemes are proposed, and their applications for both best-effort PU interference mitigation and hard interference temperature (IT) constraints are shown.
- When PU CSIT is completely unknown to a CBS, two computationally efficient SU selection schemes based on modified spatial water-filling (SWF) methods are proposed.

This scenario does not appear to have been considered previously in cognitive radio (CR) user selection.

- In an uplink (UL) system of the cellular users who are coexisting with a device-to-device network, the proposed scheduling shows better quality of service (QoS). At the same time, the interference to device-to-device user equipment is reduced, which improves the data rate.

- The eNB, C-UE, and D2D UE are all assumed to be equipped with multiple antennas, unlike that in other work [15]-[29].

- No knowledge is assumed regarding the interfering cross-channels or interference levels from C-UE to D2D UE; instead, the C-UE performs a best-effort interference mitigation.

The remainder of this work is organized as follows. The MIMO cognitive radio network and the MIMO D2D cellular network model are introduced in Chapter. 2. The proposed user selection and power allocation (PA) schemes are introduced in Chapter. 3. The UL C-UE scheduling method with best-effort interference mitigation to the D2D UE is described in Chapter 4. Several simulation results are shown in Chapter. 5, followed by conclusions in Chapter. 6.

Notation: Uppercase boldface and lowercase boldface letters denote matrices and vectors. The Frobenius and Euclidean norms of matrix $\mathbf{A}$ are denoted by $\|\mathbf{A}\|_F$ and $\|\mathbf{A}\|$, respectively. $\mathbf{A}^{\mathcal{H}}$ represents the conjugate transpose of matrix $\mathbf{A}$, $|\mathcal{A}|$ is the cardinality of the set $\mathcal{A}$, and $\mathcal{CN}(\mathbf{0}, \mathbf{Z})$ denotes a complex Gaussian random vector with zero mean and covariance matrix $\mathbf{Z}$.

CHAPTER 2

SYSTEM MODEL

Consider a downlink MIMO CR network with a t-antenna CBS, a set $\mathcal{K}$ comprising K SUs with r multiple antennas each, and a PU with r_p receive antennas as well as t_p transmit antennas. Figure 2.1 shows a block diagram of the system model considered. This dissertation assumes that it is possible to have multiple primary transmitter-receiver pairs, as shown in Figure 2.1, but each PU pair uses different carrier frequencies, and the PU transmitter (TX) and PU receiver (RX) are not co-located. A PU RX only receives and does not transmit. Interference from the CBS to another primary user receiver, say PU$'$ RX, and interference from the PU$'$ TX to the desirable SU RXs will be negligible because of different carriers. Hence, the focus here is on only a single pair of PU TX and PU RX, as shown in Figure 2.1. The CBS selects C out of K total SUs for simultaneous downlink transmission. The CBS transmit signal and the received signal at SU_k can be written, respectively, as $\mathbf{x}_s = \sum_{j=1}^{C} \mathbf{W}_j \mathbf{u}_j$, and

$$\mathbf{y}_k = \mathbf{H}_k \mathbf{x}_s + \mathbf{n}_k = \mathbf{H}_k \mathbf{W}_k \mathbf{u}_k + \sum_{j=1, j\neq k}^{C} \mathbf{H}_k \mathbf{W}_j \mathbf{u}_j + \mathbf{n}_k \tag{2.1}$$

where $\mathbf{W}_k \in \mathbb{C}^{t \times l_k}$ is the linear precoding matrix, $\mathbf{H}_k$ is the $(r \times t)$ complex channel matrix from the CBS to the k^{th} SU RX with i.i.d $\mathcal{CN}(0,1)$ components, $\mathbf{u}_k$ $(l_k \times 1)$ is the desired signal vector with $E\left\{\mathbf{u}_k \mathbf{u}_k^{\mathcal{H}}\right\} = \mathbf{I}_{l_k}$, and $\mathbf{n}_k \sim \mathcal{CN}(\mathbf{0}, \mathbf{Z}_k)$ is a additive colored Gaussian noise vector including interference from the PU TX to the k^{th} SU RX. No cooperation between the CBS and PU is assumed. The CBS obeys a total average transmit power constraint of P_{tot} and employs the block diagonalization (BD) precoding scheme for the scheduled SUs [39], which eliminates all inter-SU interference. It is assumed that the CBS has perfect CSIT $\mathbf{H}_j$ of all SUs, so that the BD precoding design, i.e., $\mathbf{H}_k \mathbf{W}_j = \mathbf{0}, j \neq k$, yields

$$\mathbf{y}_k = \mathbf{H}_k \mathbf{W}_k \mathbf{u}_k + \mathbf{n}_k. \tag{2.2}$$

The k^{th} scheduled SU has a minimum required spectral efficiency of R_k bits/s/Hz, $k = 1, \ldots, C$, and its transmit covariance matrix is $\mathbf{Q}_k = \mathbf{W}_k \mathbf{W}_k^H$.

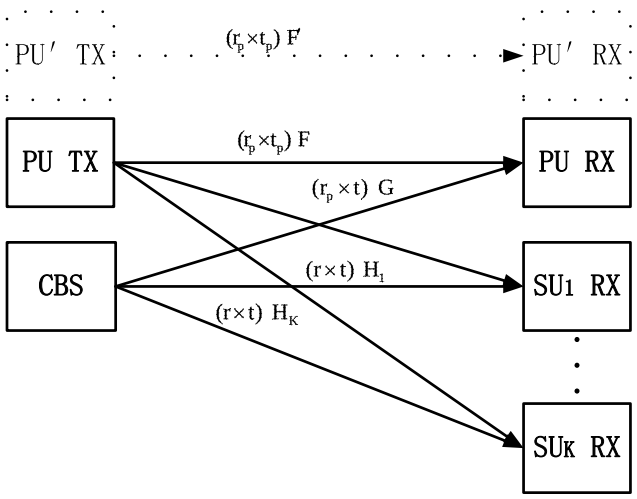

Figure 2.1: System model of MIMO CR network.

On the other hand, the received signal at the PU RX is

$$\mathbf{y}_p = \mathbf{F}\mathbf{x} + \mathbf{G}\sum_{k=1}^{C} \mathbf{W}_k \mathbf{u}_k + \mathbf{n}_p, \tag{2.3}$$

where $\mathbf{F}$ is the primary channel matrix, $\mathbf{x}$ is the desired primary data vector with covariance matrix $\mathbf{Q}_p$, $\mathbf{G}$ is the $(r_p \times t)$ interfering cross-channel matrix from the CBS to the PU RX, and $\mathbf{n}_p \sim \mathcal{CN}(\mathbf{0}, \mathbf{Z}_p)$ is an AWGN vector. In both cases of perfectly known primary CSIT and unknown primary CSIT, the channel state information (CSI) $\mathbf{H}_k$ from the CBS to the k^{th} SU is known to the CBS $(k = 1, \ldots, K)$, and the difference between the two cases is whether the CBS has knowledge of the interference channel $\mathbf{G}$ from the CBS to the PU RX or not. In either case, the PU TX has no knowledge of the cross-channel matrix $\mathbf{G}$. The analysis and conclusions in this dissertation are still valid regardless of whether the CSI $\mathbf{F}$ from the PU TX to the PU RX is available at the PU TX or not. The SU selection scheme for the unknown primary CSIT case is, in fact, independent of the number of PU receivers.

The CBS is required to avoid interfering with the PU RX as much as possible [8]. Generally in an underlay CR operation, the interference temperature is considered to be an important criterion of system performance. Here, the IT at the PU RX is

$$T_p = \mathrm{Tr}(\mathbf{G} \sum_{j=1}^{C} (\mathbf{W}_j \mathbf{W}_j^{\mathcal{H}}) \mathbf{G}^{\mathcal{H}}). \tag{2.4}$$

Consequently, the data rate of the PU can be computed as [36, 39]

$$R_p = \log_2 \det(\mathbf{I} + \mathbf{F}\mathbf{Q}_p\mathbf{F}^{\mathcal{H}}(\mathbf{Z}_p + \mathbf{G} \sum_{j=1}^{C} \mathbf{Q}_j \mathbf{G}^{\mathcal{H}})^{-1}). \tag{2.5}$$

For the system of MIMO cellular users coexisting with a MIMO D2D network users, the uplink of a cellular network coexisting with an underlay D2D network is considered, as shown in Figure 2.2. The cellular network contains C C-UE with data to be transmitted to the eNB, while the D2D network contains M active D2D UE pairs, with each pair comprising a D2D UE communicating with a single partner D2D UE. The eNB, C-UE, and D2D UE have N_e, N_c, and N_d antennas, respectively. Subchannel i has an average transmit power constraint of P_i, $i = 1, \ldots, C + M$. The uplink band is divided into K total subchannels forming set $\mathcal{K}$ out of them K' subchannels form a resource pool $\mathcal{K}_d$ ($\mathcal{K}_d \subset \mathcal{K}$, $|\mathcal{K}_d| = K'$) that may be used by D2D UE. It is assumed that D2D UE cannot simultaneously transmit to the eNB, and C-UE does not simultaneously engage in D2D communication.

The resource selection by the D2D UE is autonomous, i.e., they randomly select subchannels from $\mathcal{K}_d$ for transmission of D2D discovery and data signals. On the other hand, the uplink resource allocation of the C-UE is controlled by the eNB. The allocation problem faced by the eNB is whether any C-UE should also be scheduled within $\mathcal{K}_d$ and if so, which C-UE. This problem is rendered more difficult due to the following assumptions:

- The eNB does not know the interference (CSI) from C-UE to D2D UE. Here, D2D UEs and C-UEs behave the PUs and the SUs, respectively. And the eNB takes a role of CBS.

- The eNB does not know which D2D UE is using which subchannels within $\mathcal{K}_d$.

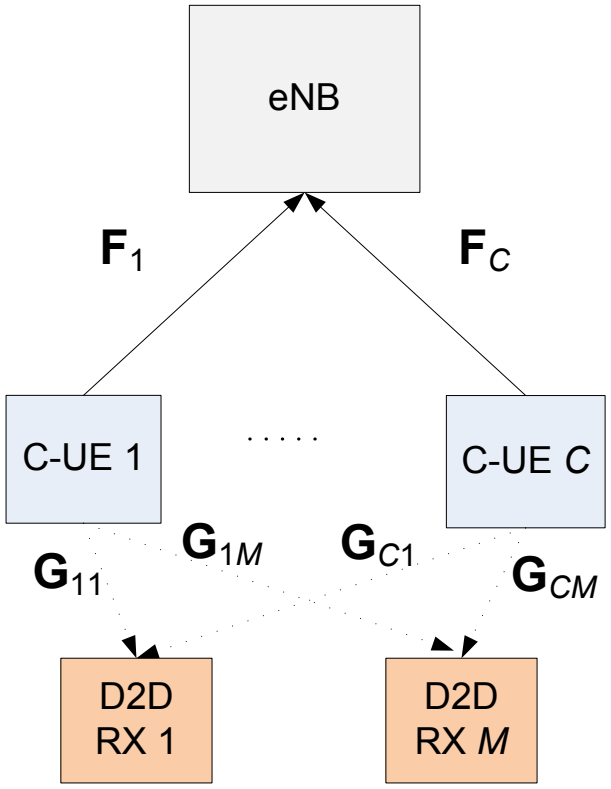

Figure 2.2: C-UE uplink with D2D underlay network.

The binary indicator variable p_i^k is defined as

$$p_i^k = \begin{cases} 1 & \text{if C-UE } i \text{ is allocated subchannel } k \\ 0 & \text{otherwise.} \end{cases} \tag{2.6}$$

Any subchannel in the system is allocated to, at most, one C-UE to avoid intra-C-UE uplink interference, which implies $\sum_{i=1}^{C} p_i^k \leq 1 \forall k \in \mathcal{K}$ where C is the number of C-UEs. Let each D2D transmitter-receiver pair share a common index j, $j = 1, \ldots, M$. Furthermore, denote d_j^k as a binary indicator variable with value $d_j^k = 1$, if D2D UE j is active on subchannel j, and $d_j^k = 0$, otherwise. Note that $d_j^k = 0 \forall k \notin \mathcal{K}_d$. It is assumed that D2D UE employs a cognitive channel selection mechanism such that intra-D2D interference is negligible. Detailed procedures for how the D2D UEs autonomously choose operating subchannels are out of the scope of this work.

The received signal at an arbitrary D2D UE j on subchannel $k' \in \mathcal{K}_d$ can be written as

$$\mathbf{y}_j(k') = \mathbf{H}_j(k')\,\mathbf{s}_j(k') + \sum_{i=1, i\neq j}^{C} p_i^{k'}\mathbf{G}_{ij}(k')\,\mathbf{z}_i(k') + \mathbf{n}_j(k') \tag{2.7}$$

where k' is chosen autonomously by the D2D UE, and hereafter suppresses the subchannel index, $\mathbf{H}_j$ is the $(N_d \times N_d)$ complex flat-fading channel matrix from the intended D2D source that transmits signal vector $\mathbf{s}_j \in \mathbb{C}^{(N_d \times 1)}$, $\mathbf{G}_{ij}$ is the $(N_d \times N_c)$ interference channel matrix from C-UE i that transmits $\mathbf{z}_i \in \mathbb{C}^{(N_c \times 1)}$ to the j^{th} selected D2D UE, and $\mathbf{n}_j \sim \mathcal{CN}(\mathbf{0}, \sigma_j^2\mathbf{I})$ is complex zero-mean circular symmetric Gaussian noise vector. D2D signals have the transmit covariance matrix $E\left\{\mathbf{s}_j(k)\,\mathbf{s}_j^H(k)\right\} = \mathbf{X}_j(k)$.

On the other hand, the matching of C-UE to uplink subchannels is controlled by the eNB through p_i^k. The received signal at the eNB on subchannel k is written as

$$\mathbf{r}(k) = \sum_{i=1}^{C} p_i^k\mathbf{F}_i(k)\,\mathbf{z}_i(k) + \sum_{j=1}^{M} d_j^k\mathbf{E}_j(k)\,\mathbf{s}_j(k) + \mathbf{w}(k) \tag{2.8}$$

where suppressing the subchannel index, $\mathbf{F}_i$, is the $(N_c \times N_e)$ complex flat-fading channel matrix from the C-UE to the eNB, $\mathbf{E}_j$ is the interfering $(N_d \times N_c)$ cross-channel matrix from the D2D transmitter j, and $\mathbf{w} \sim \mathcal{CN}(\mathbf{0}, \sigma_e^2\mathbf{I})$ is the complex zero-mean circular symmetric Gaussian noise vector. C-UE signals have the transmit covariance matrix $E\left\{\mathbf{z}_i(k)\,\mathbf{z}_i^H(k)\right\} = \mathbf{Q}_i(k)$. It is assumed that the i^{th} C-UE waiting to be scheduled has a data rate requirement of $\bar{R}_i$ bits/s. C-UE may be assigned multiple subchannels, but is constrained to use the same number of spatial streams, denoted by n_i, $i = 1, \ldots, C$, on each. The overall achieved data rate for C-UE i is

$$R_i = \sum_{k=1}^{K} p_i^k W \log_2\left|\mathbf{I} + \mathbf{F}_i(k)\,\mathbf{Q}_i(k)\,\mathbf{F}_i^H(k)\,\mathbf{T}(k)^{-1}\right| \tag{2.9}$$

where

$$\mathbf{T}(k) = \sigma_e^2\mathbf{I} + \sum_{j=1}^{M} d_j^k\mathbf{E}_j(k)\,\mathbf{X}_j(k)\,\mathbf{E}_j^H(k) \tag{2.10}$$

is the received interference-plus-noise covariance matrix on subchannel k at the eNB and $\mathbf{X}_j(k) = E\{\mathbf{s}_j(k)\mathbf{s}_j^H(k)\}$.

CHAPTER 3

MIMO COGNITIVE RADIO USER SELECTION

Assume that the CBS wishes to select a subset $\mathcal{U} \subseteq \mathcal{K}$ of size C out of K possible total SUs. In the conventional multi-antenna downlink with single-antenna users and no PUs, a semi-orthogonal user selection (SOUS) scheme provides the same asymptotic sum capacity as dirty paper coding when the number of users approaches infinity [31]. This is because the SOUS algorithm schedules receivers with near-orthogonal channels, which ensures that the resulting downlink channel is well-conditioned and conducive to channel inversion (zero forcing) when there are a large number of users from which to choose. In [32], the SOUS algorithm was extended to a MIMO downlink with BD precoding but without PUs. Heuristic user selection strategies for sum-rate maximization in a conventional MIMO downlink with BD precoding were studied by Shen et al. [33].

In this dissertation, we will examine two different philosophies for CBS-to-PU interference mitigation during SU scheduling. In the first case, best-effort interference mitigation is adopted in the sense that no hard IT constraint is assumed, even if the primary CSIT $\mathbf{G}$ is available at the CBS, which is similar that of other work [8, 34, 35]. This is justifiable, for example, when the CBS lies outside a primary exclusion area or guard zone, or the maximum CBS transmit power is designed based on a worst-case PU interference scenario. Note that only best-effort interference mitigation is possible when PU CSIT $\mathbf{G}$ is completely unknown. In the second case, a hard IT constraint is enforced when PU CSIT $\mathbf{G}$ is known to the CBS, similar to the majority of prior work on underlay CR systems.

3.1 Perfect Primary CSIT G at CBS

We first assume that cross channel $\mathbf{G}$ from the CBS to a PU is known to the CBS, which is feasible if channel reciprocity can be exploited, as in time-division duplex systems. A first approach could be to enforce a BD constraint for the PU such that $\mathbf{G}\mathbf{W}_k = 0$ $\forall k$. However, this approach suffers from a transmit power-boosting problem when $\mathbf{G}$ is ill-

conditioned, resulting in performance degradation for the SUs. More importantly, it may not always be feasible to completely zero-force the interference to the PU, for example, when the PU has more antennas than the CBS.

Two heuristic scheduling approaches for this scenario are proposed: (1) channel similarity-based user selection (CSUS) and (2) precoder-based group user selection (PGUS). For both methods, an explanation is offered for how the CBS selects $C(\leq K)$ SUs to make a best-effort attempt to avoid interference with the PU, which is the same philosophy as in Hamdi et al. [8].

For CSUS, the interest here is in selecting SUs whose channel matrices $\mathbf{H}_j$ are as dissimilar as possible to the PU cross-channel $\mathbf{G}$. The metric $\|(\mathbf{G} - \mathbf{H}j)\|_F$ can serve as a dissimilarity measure. For example, $\|(\mathbf{G} - \mathbf{H}_j)\|_F \gg 0$ would represent a high-dissimilarity case, which is desirable, but the case with $\|(\mathbf{G} - \mathbf{H}_j)\|_F = 0$ would be undesirable. This is because if $\|(\mathbf{G} - \mathbf{H}_j)\|_F$ approaches zero, then $\mathbf{G}$ will approach $\mathbf{H}_j$ also. Hence, $\|\mathbf{H}_j\mathbf{W}_j\|_F$ would be approximately equal to $\|\mathbf{G}\mathbf{W}_j\|_F$. But $\|\mathbf{G}\mathbf{W}_j\|_F$ is related to interference from the j^{th} SU signal in the CBS to the PU RX. However, the j^{th} SU precoder $\mathbf{W}_j$ should be designed generally to make $\|\mathbf{H}_j\mathbf{W}_j\|_F$ large to ensure that the data rate is high; hence, the interference to the PU RX would be also be large. Although $\|(\mathbf{G} - \mathbf{H}_j)\|_F$ can serve as a dissimilarity measure, the dimensions of $\mathbf{G}$ and $\mathbf{H}_j$ are $(r_p \times t)$ and $(r \times t)$ respectively, and they can be different from each other in general. Hence, instead of employing $\|(\mathbf{G} - \mathbf{H}_j)\|_F$, the following definition is used to quantify the dissimilarity between two matrices $\mathbf{G}$ and $\mathbf{H}_j$ as

$$S\left(\mathbf{G}, \mathbf{H}_j\right) = \left\|(\mathbf{G}^{\mathcal{H}}\mathbf{G} - \mathbf{H}_j^{\mathcal{H}}\mathbf{H}_j)\right\|_F. \tag{3.1}$$

This metric is also valid even for different dimension cases. In other words, equation (3.1) is valid even when the PU and SUs have a different number of receiving antennas. If $\mathbf{G} = \mathbf{H}_j$, then $S(\mathbf{G}, \mathbf{H}_j)$ is zero, i.e., zero dissimilarity, although this is not true for the vice vice-versa, and when $S(\mathbf{G}, \mathbf{H}_j)$ gets larger, the dissimilarity also gets larger. We cannot prove that the

dissimilarity metric in equation (3.1) is optimal, but it can serve as a dissimilarity measure as $\|(\mathbf{G} - \mathbf{H}_j)\|_F$.

To select appropriate SUs in CSUS, we adopt a two-stage user-selection method. First, SUs that satisfy $S(\mathbf{G}, \mathbf{H}_n) > \alpha_p$ for a small positive number $\alpha_p \geq 0$ are preselected, which is similar to the SOUS approach in the work of Hamdi et al. [8]. Then, the SU with the highest channel Frobenius norm is selected as the first SU. In the second stage, to find the remaining $(C-1)$ SUs, equation (3.1) is applied again between preselected and already-selected SU channels. SUs satisfying $S(\mathbf{H}_n, \mathbf{H}_{selected}) > \alpha_c$ are selected, and the SU with the highest channel Frobenius norm is chosen from them. This second stage continues until C SUs are selected, followed by precoder computation and power allocation to achieve the desired SU rates R_k. Details of the proposed CSUS scheme are shown in Algorithm 1, where α_p and α_c need to be chosen to guarantee that there are sufficient SU candidates in both stages 1 and 2. In Chapter 5, these thresholds are obtained numerically. The CSUS scheme is also applicable when $\mathbf{G}$ is partially known, such as its line-of-sight component only. In practice, when C number of SUs out of K are selected, there are $\binom{K}{C}$ possible combinations. Among these, there are at least one optimal combination and one worst combination. In an optimal combination, the channel matrices $\mathbf{H}_j$ of the selected C SUs are highly dissimilar to the cross-channel interference matrix $\mathbf{G}$. Hence, interference from the CBS to the PU RX would be small, and the PU data rate can be high. In contrast, in a worst combination, the SU channel matrices $\mathbf{H}_j$ are similar to G, which may cause high interference, and the PU data rate can be low. The PU data rate versus the SU data rate are similar for the worst and the best combinations when channel matrices $\mathbf{H}_j$ are generated randomly and fixed using Algorithm 3 (i.e., unknown CSIT G), $j = 1, 2, ...K(= 20)$ and $C = 3$. Here, an exhaustive search was used to find the best and worst combination cases for the given set of channels. Using the proposed combination and power allocation Algorithm 3, it can be observed that the proposed algorithm performs close to the best case and better than the worst combination which will be shown in Chapter 5.

Algorithm 1 Channel similarity-based user selection (CSUS).

$\mathcal{U} = \emptyset, \mathcal{V} = \emptyset, \mathcal{V}_c = \emptyset$
for $n, \forall\ \mathrm{SU}_n \in \mathcal{K}$ **do**
    Calculate : $\gamma(n) = S(\mathbf{G}, \mathbf{H}_n), \theta(n) = \|\mathbf{H}_n\|_F$
end for
$M = \{\mathrm{SU}_n : \gamma(n) > \alpha_p\}, \mathcal{V} = \mathcal{V} + M$
$N_{selected} = \arg \max_{n:\mathrm{SU}_n \in \mathcal{V}} (\theta(n)), \mathcal{U} = \mathcal{U} + \mathrm{SU}_{N_{selected}}, \mathcal{V} = \mathcal{V} - \mathrm{SU}_{N_{selected}}$
while $|\mathcal{U}| < C$ **do**
    $\mathcal{V}_c = \{\mathrm{SU}_n : S(\mathbf{H}_n, \mathbf{H}_k) > \alpha_c, \forall\ \mathrm{SU}_n \in \mathcal{V}, \mathrm{SU}_k \in \mathcal{U}\}$
    $N_{selected} = \arg \max_{n:\mathrm{SU}_n \in \mathcal{V}_c} (\theta(n)), \mathcal{U} = \mathcal{U} + \mathrm{SU}_{N_{selected}}, \mathcal{V} = \mathcal{V} - \mathrm{SU}_{N_{selected}}$
end while

For the PGUS scheme, unlike SOUS and CSUS, orthogonality between the primary channel $\mathbf{G}$ and SU precoder matrices $\{\mathbf{W}_k\}_{k=1}^K$ is of greater interest. For any two matrices $\mathbf{G}$ and $\mathbf{W}_j$, their orthogonality is quantified as

$$T(\mathbf{G}, \mathbf{W}_j) = \|\mathbf{G}\mathbf{W}_j\|_F. \tag{3.2}$$

Thus reducing $T(\mathbf{G}, \mathbf{W}_j)$ will reduce the PU IT in equation (2.4). To achieve this, the best SU index should be selected as:

$$N_{selected} = \underset{j}{\mathrm{argmin}}(T(\mathbf{G}, \mathbf{W}_j)). \tag{3.3}$$

However, note that under BD, the precoder matrix $\mathbf{W}_k$ is derived from the singular value decomposition (SVD) of other SU channels excluding SU k, and thus equation (3.3) cannot be evaluated directly. If an exhaustive search is applied to find the best set of C SUs that minimizes equation (2.4), this would entail checking all $\binom{K}{C} = \frac{K!}{C!(K-C)!}$ combinations and their corresponding BD precoder computations. An exhaustive search, therefore, involves formidable complexity. The proposed PGUS scheme is a suboptimal but much simpler method, which relies on the notion of a "sliding window" SU search. Instead of searching all $\binom{K}{C}$ combinations, only certain combinations are screened. Out of K total SUs, only $(K-C+1)$ combinations will be screened, where the i^{th} combination includes SU_i to SU_{i+C-1}, which is called the i^{th} sliding window group. For each sliding window group containing C

SUs, upon finding precoder matrices $\mathbf{W}_k$ for each member, the cumulative orthogonality measure of the group can be calculated as

$$\beta(n) = \sum_{j=1}^{C} T(\mathbf{G}, \mathbf{W}_{j+n-1}) \tag{3.4}$$

where $\beta(n)$ represents the orthogonality of the n^{th} sliding window group. The best sliding window group will be selected based on

$$N_{selected} = \underset{n}{\operatorname{argmin}}(\beta(n)) \tag{3.5}$$

where $N_{selected}$ is the index of the selected group as well as the index of the first SU in the group. Selecting a group means that all members of the group are selected. The proposed PGUS algorithm is detailed in Algorithm 2. Similar to CSUS, the optimal and worst combination a are in the total $\binom{K}{C}$ combinations. Because the selection to $K - C + 1$ "sliding window" combination groups has been narrowed down, the optimal combination will be one of the sliding window groups. However, it is not possible to select the worst combination group since the scheme will always select the best combination group out of the $K - C + 1$ "sliding window" combination groups. The worst-case scenario would be the sliding window groups consisting of worst $K - C - 1$ combinations among all $\binom{K}{C}$ combinations. Similar to Algorithm 1, it is less likely that this selection will fall into the two extreme cases: either the optimal or worst combination when K is large.

Algorithm 2 Precoder-based group user selection (PGUS) with sliding window search method.

1: **for** $n \leftarrow 1 : K - C + 1$ **do**
2: Candidates are : SU_n, SU_{n+1}... SU_{n+C-1}, Calculate : $\mathbf{W}_n, \mathbf{W}_{n+1}...\mathbf{W}_{n+C-1}$
3: $\beta(n) = \sum_{j=n}^{n+C-1} T(\mathbf{G}, \mathbf{W}_j)$
4: **end for**
5: $N_{selected} = \underset{n}{\operatorname{argmin}}(\beta(n))$
6: Select : $\mathrm{SU}_{N_{selected}}, \mathrm{SU}_{N_{selected}+1}, ...\mathrm{SU}_{N_{selected}+C-1}$

Thus far, CSUS and PGUS have been presented from the perspective of best-effort

PU interference mitigation. It is evident that with minor modifications, they can also be used in the case when a hard limit on the PU IT must be observed by the CBS. For example, in PGUS, modification would be in the choice of the PGUS sliding window group size, which is initialized as two instead of starting with a window size of C. The sliding window size is gradually incremented by 1 until either the maximum IT constraint is reached or C SUs have been selected.

3.2 No Primary CSIT G at CBS

The worst-case scenario from the perspective of interference avoidance to the PU is when the CBS has completely no knowledge of its CSI $\mathbf{G}$, i.e., the realization and probability distribution of $\mathbf{G}$ are unknown. This case is more realistic when PU and SU networks have different air interfaces and do not cooperate, but this has not been studied much in the literature. Without knowledge of $\mathbf{G}$, the CBS cannot limit the PU IT to any predefined threshold. However, best-effort interference mitigation is still possible by intelligently designing the spatial PA for the SUs. In the work of Pei et al. [36], for a point-to-point SU MIMO system it was shown that reducing the number of spatial dimensions, which are allocated non-zero transmit power, reduces PU interference, compared to classical water-filling (CWF), which seeks to reduce the SU transmit power needed to achieve a desired rate. The benefits of coordinating transmission rank for interference mitigation have also been observed in multi-cell MIMO-OFDMA networks [37].

Motivated by this, two selection schemes are proposed for the downlink CR network based on the following: (1) frugal water-filling (FWF), and (2) balanced water-filling (BWF) [36, 38]. The idea behind FWF is to minimize the rank of the transmit covariance matrix of each SU, but it generally requires much higher transmit power compared to CWF. To be more balanced in terms of transmit power and rank, BWF is also utilized in this dissertation and seeks to minimize the product of the transmit covariance matrix rank and the required transmit power. In the context of BD precoding, by letting $\mathbf{W}_k = \mathbf{T}_k \mathbf{\Lambda}_k^{1/2}$, it is possible to separately design the beamforming matrix $\mathbf{T}_k$ and diagonal PA matrix $\mathbf{\Lambda}_k$ per user to achieve

rate R_k in a two-step process. While BD precoders are designed using the conventional approach [39], controlling the rank of $\mathbf{\Lambda}_k$ is the key idea behind PU interference mitigation in the no-CSIT scenario. Let $r_k = \text{rank}(\mathbf{H}_k\mathbf{T}_k)$ for the SU k's effective channel, and assume the desired signal vector dimension $l_k = r_k$. Consider the SVD of user k's pre-whitened effective channel as

$$\mathbf{Z}_k^{-1/2}\mathbf{H}_k\mathbf{T}_k = \mathbf{U}_k\mathbf{\Lambda}_k\mathbf{V}_k^{\mathcal{H}}$$

where $\mathbf{Z}_k$ is the colored noise covariance matrix, and $\mathbf{\Lambda}_k = \text{diag}\left(\lambda_{k,1}, \ldots, \lambda_{k,r_k}\right)$ is the PA matrix. While Spencer et al. [39] computed $\mathbf{\Lambda}_k$ using CWF in order to minimize the power required to achieve rate R_k, in this dissertation, the alternative FWF and BWF schemes are applied instead. Due to the subadditivity of the rank function, reducing the rank of the per-user transmit covariances via FWF effectively reduces the rank of the overall CBS transmit covariance $\mathbf{Q}_{CBS} = \sum_{j=1}^{C} \mathbf{Q}_j$. The BWF discussed earlier can also be applied for SU selection by considering both power and rank for a better tradeoff between the two.

For selection with FWF, the best SU index at each round will be selected as

$$N_{selected} = \underset{k}{\text{argmin}}(\text{rank}(\mathbf{Q}_k)), \tag{3.6}$$

whereas for BWF, the best SU index will be selected as

$$N_{selected} = \underset{k}{\text{argmin}}(\text{rank}(\mathbf{Q}_k)\,\|\mathbf{Q}_k\|_F). \tag{3.7}$$

To efficiently find $\{\mathbf{W}_k\}$ for different sets of potential candidate SUs, the same complexity issue as discussed for the PGUS arises. A suboptimal successive search method to simplify screening. Two steps are included in this searching method. The first step is to search for the initial SU, where $\mathbf{T}_k = \mathbf{I}$ is set during the first step search. In this way, the covariance matrix of the k^{th} SU is $\mathbf{Q}_k = \mathbf{\Lambda}_k\mathbf{\Lambda}_k^{\mathcal{H}}$, which can be easily found. Then the first SU can be selected by applying either the FWF or BWF criterion. The second step is to continue searching the subsequent SUs after the initial selection. In this step, zero-forcing is applied only to the previously selected SUs. For example, when selecting the third SU,

zero-forcing is only applied to the first and second selected SUs. Once $\mathbf{Q}_k$ is found, the next SU is selected using either FWF or BWF. A similar approach with classical water-filling was used in the work of Shen et al. [33]; however, PUs were not considered. The proposed algorithm of water-filling using successive search is shown in Algorithm 3.

Algorithm 3 Water-filling with suboptimal successive search (CWF, FWF, and BWF).

T

$\mathcal{U} = \emptyset$
while $|\mathcal{U}| < C$ **do**
    if CWF **then**
        for $n, \forall$ SU$_n \in \mathcal{K}$ **do**
            Calculate $\mathbf{W}_n$, where $\mathbf{H}_j \mathbf{W}_n = 0, \forall$ SU$_j \in \mathcal{U}$
            Calculate total power $P(n)$, where $P(n) = \left\| \mathbf{Q}_n \mathbf{Q}_n^{\mathcal{H}} \right\|, \forall$ SU$_n \in \mathcal{U}$
        end for
        $N_{selected} = \underset{n}{\operatorname{argmin}}(P(n))$
    else if FWF **then**
        for $n, \forall$ SU$_n \in \mathcal{K}$ **do**
            Calculate $\mathbf{W}_n$, where $\mathbf{H}_j \mathbf{W}_n = 0, \forall$ SU$_j \in \mathcal{U}$
            Calculate $R(n) = \operatorname{rank}(\mathbf{Q}_n)$ of candidate n.
        end for
        $N_{selected} = \underset{n}{\operatorname{argmin}}(R(n))$
            ▷ **If** $|\{j : R(n) = \min(R(n))\}| > 1$, then $N_{selected} = \arg \underset{j:R(j)=\min_n(R(n))}{\max} \|\mathbf{H}_j\|$
    else if BWF **then**
        for $n, \forall$ SU$_n \in \mathcal{K}$ **do**
            Calculate $\mathbf{W}_n$, where $\mathbf{H}_j \mathbf{W}_n = 0, \forall$ SU$_j \in \mathcal{U}$
            Calculate $B(n) = P(n) \times R(n)$ of candidate n.
        end for
        $N_{selected} = \underset{n}{\operatorname{argmin}}(B(n))$
    end if
    $\mathcal{U} = \mathcal{U} + \text{SU}_{N_{selected}}, \mathcal{K} = \mathcal{K} - \text{SU}_{N_{selected}}$
end while

3.3 Power Allocation with Primary CSIT G at CBS

It is assumed that each of the selected SUs obeys the individual transmit power constraint $P_{SU} = P_{tot}/C$. When CSIT $\mathbf{G}$ is available at the CBS and C SUs are selected using either CSUS or PGUS, the CWF PA for each SU and the temporary data rate R_{temp}

is obtained for the k^{th} SU. It is possible that $R_{temp} > R_k$, which means that the k^{th} SU performs better than the requirement, and it is not necessary for the k^{th} SU to transmit with full power P_{SU}. To reduce interference from the CBS to the PU RX, the transmit power of the k^{th} SU is lowered to P_k until the new data rate for the k^{th} SU R_{temp} approaches R_k.

3.4 Power Allocation with No Primary CSIT G at CBS

Similar to the power allocation method discussed in section 3.3, each SU's transmit power is initially constrained to P_{SU} when the CSIT $\mathbf{G}$ is not available. To apply the FWF PA for the k^{th} SU, first, P_{SU} is assigned to the strongest channel component, i.e, the largest eigenvalue. This means that the rank of the k^{th} SU transmitting covariance matrix $\mathbf{Q}_k$ becomes one. A temporary data rate R_{temp} is calculated. Then $R_{temp} < R_k$ may be possible if SU k is not able to achieve R_k by using only one independent channel component. Hence, the number of independent channel components is increased to n_k until $R_{temp} \approx R_k$. The term n_k is the minimum number of independent channel components for the k^{th} SU to achieve R_k. Furthermore, the power constraint assigned to n_k independent channel components is attempted to be reduced to P_k so that $R_{temp} \approx R_k$. The BWF PA procedures are similar to those of the FWF. Instead of finding n_k, the minimum product value of the number of used channel components, i.e, the $rank(\mathbf{Q}_k)$ and the minimum transmitting power for the k^{th} SU are attempted to be found. Note that the CWF, FWF, and BWF PA methods described in sections 3.3 and 3.4 are part of the user-selection schemes. Because CWF, FWF, and BWF user selections are based on each SU's minimum transmitting power, minimum rank of $\mathbf{Q}_{CBS}$, and minimum product of transmitting power and rank of $\mathbf{Q}_{CBS}$, respectively, then CWF, FWF, and BWF are not named separately for user selection and power allocation. However, the methods and power-allocation methods can be combined into hybrid schemes. For example, the CSUS can be combined with BWF, which is expected to outperform CWF PA, as described in 3.3.

3.5 Computational Complexity

The suboptimal scheduling methods presented above decrease the computational complexity significantly compared to a brute-force search, as quantified further in this section.

3.5.1 Perfect Primary CSIT

In the CSUS, step $\mathbf{G}^{\mathcal{H}}\mathbf{G}$ needs $tr_p + (6r_p - 2)t^2$ required flops. In the first stage, for each SU, $\mathbf{H}_k^{\mathcal{H}}\mathbf{H}_k$ has $tr + (6r - 2)t^2$ flops, $\left\|\mathbf{G}^{\mathcal{H}}\mathbf{G} - \mathbf{H}_k^{\mathcal{H}}\mathbf{H}_k\right\|_F$ has $6t^2$ flops, and $\|\mathbf{H}_k\|_F$ has $2tr$ flops. In the second stage, assume $N_{\mathcal{V}}$ SUs are in $\mathcal{V}$ of Algorithm 1. To calculate $S(\mathbf{H}_n, \mathbf{H}_k)$ in step 8, $\frac{(2N_{\mathcal{V}}-C)(C-1)}{2}6t^2$ flops are needed. Since $K \gg C$, the total number of flops for the CSUS selection is

$$\psi_c = ((6r+4)t^2 + 3tr)K + ((6r_p - 2)t^2 + tr_p) + \frac{(2N_{\mathcal{V}} - C)(C-1)}{2}6t^2 \approx \mathcal{O}(Krt^2). \quad (3.8)$$

In the PGUS, assume that C is properly chosen. Then the computational complexity is derived in a similar way as [33]. For each sliding window group member, to find $\mathbf{T}_k$ using SVD requires $48(C-1)^2r^2t + 24(C-1)rt^2 + 54(C-1)^3r^3$ flops. Determining $\mathbf{H}_k\mathbf{T}_k$ requires $8tr(t-(C-1)r)$ flops, and to operate SVD on it requires $48r^2(t-(C-1)r) + 24r(t-(C-1)r)^2 + 54r^3$ flops. Water-filling entails $2Cr(Cr+3)$ flops, and data-rate computation needs $2Cr$ flops. Since there are C members in each sliding window group and $(K-C+1)$ sliding window groups, the total number of flops needed for the PGUS is

$$\begin{aligned}\psi_p = \{&48(C-1)^2r^2t + 24(C-1)rt^2 + 54(C-1)^3r^3 + 8tr(t-(C-1)r \\ &+48r^2(t-(C-1)r) + 24r(t-(C-1)r)^2 + 54r^3 + 2Cr(Cr+3) + 2Cr\} \\ &\times C \times (K-C+1) \approx \mathcal{O}(KC^5r^3).\end{aligned} \quad (3.9)$$

Note that $\mathbf{Z}_k^{-1/2}\mathbf{H}_k\mathbf{T}_k$ in this dissertation is the equivalent SU channel instead of $\mathbf{H}_k\mathbf{T}_k$. The computational complexity does not change when using $\mathbf{H}_k\mathbf{T}_k$ as an equivalent channel just for the analysis, even though the number of flops may not be identical.

3.5.2 No Primary CSIT

For all the water-filling-based suboptimal selection methods, computational complexities can be derived in a similar way as the one in [33] as

$$\psi_w \approx \mathcal{O}(KC^5r^3). \tag{3.10}$$

Brute-force search computational complexity is derived similarly as for the PGUS. The only difference is that the number of groups is changed from $(K - C + 1)$ to $\binom{K}{C}$:

$$\psi_b \approx \mathcal{O}(\binom{K}{C}C^4r^3). \tag{3.11}$$

It is clear that our heuristic methods incur $\binom{K}{C}C^4/k$ times lesser computational complexity than an exhaustive search, since $\binom{K}{C} \gg KC$ when $K \gg 1$.

CHAPTER 4

SCHEDULING FOR DEVICE-TO-DEVICE NETWORK

By scheduling C-UE to a set of subchannels $\mathcal{K}_d$, it is expected that a greater amount of C-UE achieves its target data rates; hence, a better quality of service can be reached. Since each subchannel uses different center frequency, each C-UE experiences different CSIT for the assigned subchannels. A possible situation is that a certain subchannel is the strongest channel for C-UE A but may be the weakest for C-UE B. And bad scheduling would be assigning C-UE B into that subchannel. It will be beneficial if an optimal method for assigning C-UE to subchannels can be found. On the other hand, when C-UE is assigned to $\mathcal{K}_d$, interferences to D2D UE are occurred. Here it is important to try to keep interferences in a level so that D2D UE can maintain data transmission. This section considers D2D UEs and C-UEs as the primary users and the secondary users discussed in chapter 3, respectively.

4.1 Scheduling

It is assumed that all C-UE has one common target rate to achieve. Given that different subchannels give different CSIT as well as different channel capacity when occupied by the same C-UE, there is no straight forward way to solve the problem. The optimal solution can be found by going through all combinations of C-UE and subchannels. First a priority level is assigned to each C-UE so that any two pieces of C-UE may not share the same priority level. Scheduling begins with the C-UE with highest priority level, and eNB assigns the C-UE into the strongest channels from its point of view to reach its target data rate. Then the eNB schedules C-UE with the lower priority level until all C-UE reaches its target data rate or all subchannels are occupied by one C-UE. Since the priority level can be assigned in different ways, in order can cause a high complexity, all combinations must be tested. For C number piece of C-UE, there are $C!$ combinations, which can be very difficult to implement.

The suboptimal solution is to assign priority levels randomly the C-UE. One disad-

vantage is that the optimal solution cannot be guaranteed in such a case. However, since this is greedy scheduling, the improvement of QoS in the C-UE' service is promising. The other drawback is that when a priority level is assigned, the C-UE with a low-priority level will less likely be assigned to any subchannel. In the worst case, the C-UE with the lowest priority level may not be able to communication at all with the eNB. To solve this fairness problem, priority level assignment using random permutation can be repeatedly performed from time to time. This gives all C-UE a fair chance to be assigned to subchannels. Also random permutation may prevent the system from degradation caused by the worst-case priority level combination.

4.2 Interference Control

When C-UE is assigned to subchannels, some C-UE may be assigned to $\mathcal{K}_d$, whereby the C-UE transmissions create interference to D2D UE. It is important to control this interference in order to avoid outage of the D2D UEs in $\mathcal{K}_d$.

The basic principle behind the proposed best-effort C-UE-to-D2D UE interference mitigation mechanism is that the transmission of many spatial streams with low power is more damaging than the transmission of a few spatial streams with higher overall power. In other words, reducing the ranks of the C-UE transmit covariance matrices is preferable from the perspective of the D2D UE, even though the corresponding C-UE transmit power may be increased. As an example, Figure 4.1 shows the rate achieved by a single D2D UE when sharing a single subchannel with one C-UE, with eight antennas at both nodes. The D2D UE performs a uniform spatial power allocation with a transmit SNR of 6 dB, while the C-UE performs waterfilling over its available spatial dimensions with a rate target of $R_t = 22$ bps/Hz. In the upper part of the figure, the C-UE transmit SNR is fixed to 20 dB, and the rank of its transmit covariance matrix is varied from one to six. In the lower part of the figure, the rank of the C-UE transmit covariance matrix is fixed to three, and the C-UE transmit SNR is varied from 4 dB to 12 dB. It can be seen that a higher C-UE transmit

rank has a greater impact on the D2D UE rate, as compared to a lower transmit rank with higher C-UE transmit power.

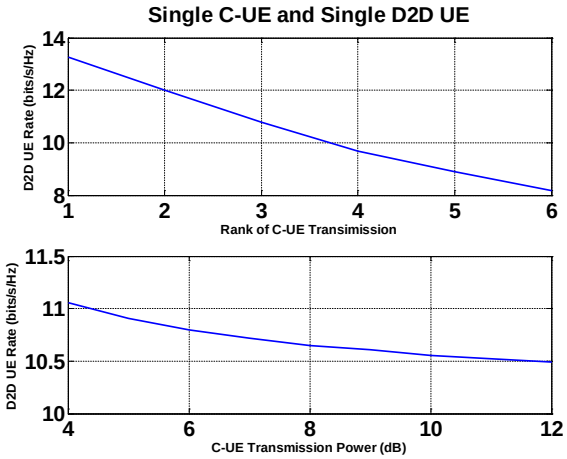

Figure 4.1: D2D UE rate paired with a single C-UE, Nc = Nd = 8.

Two modified water-filling schemes are proposed to allocate power for the MIMO system. Conventionally, water filling allocates power into all the independent channels according to each singular value obtained from a singular value decomposition of the channel. The goal of frugal water-filling is to reach a target data rate with minimal independent channel. To do that, first, only one independent channel is used by allocating all power into the strongest independent channel. The transmission data rate can be found using the corresponding power allocation matrix to check whether it is smaller than the target data rate or not. Power is allocated on more and more number of independent channels until the target data rate is achieved. The proposed FWF will eventually find the PA matrix that achieves the target data rate with the smallest rank. Balanced water-filling is used to reach the target data rate with a small number of independent channels transmissions as well as the low transmitting power. In the BWF, the same process is carried out to determine the minimal independent channel that can achieve the target data rate. Then, the number of independent channel is continually increased. After going through all the numbers of independent channel that can achieve the target data rate, the one with the lowest number

of independent channel is multiplied by the transmitting power. This detailed algorithm is shown in Algorithm 4.

Algorithm 4 Frugal Water-Filling (FWF) and Balanced Water-Filling (BWF) for i^{th} C-UE.
h

$R_i = 0, Norm_j = \|F_i(j)\|_F, j = 1, ..., K, Chosen = \varnothing$
while $R_i < \bar{R}_i$ **do**
    $R_i = 0$
    $ind = \max_j(Norm_j), Norm_{ind} = 0.$
    $Chosen = Chosen + ind.$
    $\text{Spatial}_{\text{FWF}} = 1$ $\text{Spatial}_{\text{BWF}} = 1$
    for $n = 1 : N_d$ **do**
        for $\forall m \in Chosen$ **do**
            $p_n(m) = P_m$
            Allocate $p_n(m)$ into first n spatials, obtain power allocation diagonal matrix $\Lambda_n(m)$
            $Q_i(m) = \Lambda_n(m)\Lambda_n(m)^H.$
            Calculate $R\_singlechannel_m$ using equation 2.9.
            $R_i = R_i + R\_singlechannel_m$
        end for
        if $R_i < \bar{R}_i$ **then**
            $\text{Spatial}_{\text{FWF}} + +$
        else
            Apply linesearch to reduce $p_n(m) \forall m \in Chosen$ until $R_i = \bar{R}_i$.
        end if
    end for
end while
For FWF case :
$\Lambda\_all_i(m) = \Lambda_{\text{Spatial}_{\text{FWF}}}(m) \forall m \in Chosen.$
$Q_i(m) = \Lambda\_all_i(m)\Lambda\_all_i(m)^H.$
For BWF case :
$\text{Spatial}_{\text{BWF}} = \min_n(n \sum_{m \in Chosen} p_n(m) : n \geq \text{Spatial}_{\text{FWF}}).$
$\Lambda\_all_i(m) = \Lambda_{\text{Spatial}_{\text{BWF}}}(m) \forall m \in Chosen.$
$Q_i(m) = \Lambda\_all_i(m)\Lambda\_all_i(m)^H.$

4.3 Computational Complexity Analysis

The computation load of the selection process can be very large because the number of C-UE and D2D UE is large. Hence, it becomes important to analyse the computational

complexity of these schemes. To do that, the number of flops needed for the selection process is counted. The order represents the complexity of the scheme.

The scheduling algorithm includes two steps: initial assignment and swapping adjustment. In the first step, similar conclusions can be adopted from the work of Shen et al. [33]. The Frobenius norm of $\mathbf{F}_i$ needs $4N_d^2$ flops, and there are CK frobenius norms to find. One water-filling and data-rate calculation requires

$$\psi = 48N_e^2N_c + 24N_eN_c^2 + 54N_e^3 + 2N_e^3 + 8N_e. \tag{4.1}$$

Assuming that all the subchannels are utilized at the end of scheduling. Then, the total number of flops for water-filling and data calculation is $K\psi$. The total number of flops needed for our the suboptimal step 1 is $4CKN_d^2 + K\psi$. To find the optimal solution to step 1, a complete search is necessary. This search goes through $C!$ priority level combinations. Hence the total number of flops is $C!(4CKN_d^2 + K\psi)$.

For step 2, each swap requires a water-filling and data rate calculation, which contains ψ flops. Assuming that M swaps are necessary to let the step 2 converge. Then, the total number of flops needed is $M\psi$.

In summary, for the suboptimal scheduling, the computation complexity is:

$$\begin{aligned} \psi_{sub} &= 4CKN_d^2 + K\psi + M\psi \\ &\approx \mathcal{O}(KCN_d^2). \end{aligned} \tag{4.2}$$

For the brute-force complete search, the computational complexity is:

$$\begin{aligned} \psi_{brute} &= C!(4CKN_d^2 + K\psi) + M\psi \\ &\approx \mathcal{O}(C!KCN_d^2). \end{aligned} \tag{4.3}$$

Since $C! \gg 1$, the suboptimal schedule has $C!$ lower computation complexity than the complete search.

CHAPTER 5

SIMULATION RESULTS

This chapter presents the numerical evaluations for both perfect primary CSIT and no primary CSIT scenarios. The additive white Gaussian noise vector with zero mean and covariance matrix $\mathbf{Z}_p = \sigma_p^2\mathbf{I}$ at the PU RX, uniform spatial power allocation at the PU TX, and Rayleigh fading channels are assumed. The CSUS thresholds α_p and α_c are obtained numerically to ensure that a sufficient number of candidate SUs are available in each stage.

Figure 5.1 shows the PU data rate versus the desired per-SU data rate when the primary CSIT $\mathbf{G}$ from the CBS to the PU RX is perfectly and partially known at the CBS, and the best-effort interference mitigation is pursued. Simulation conditions include PU SNR = 20 dB, $r_p = 4$, $r = 3$, $K = 20$, $C = 3, 4$, and $t = t_p = 12$. The PGUS, CSUS, conventional, and random selections were simulated, and the conventional selection was adapted from the work of Hamdi et al. [8]. In that work, the sum rate of all SUs with a MISO system were studied and simulated. For comparison, its SOUS scheme was applied to the MIMO system and the corresponding PU rate investigated. All four user-selection schemes used CWF power allocation. For perfectly known CSIT $\mathbf{G}$ at the CBS, the proposed PGUS performs the best, while the CSUS has a lower gain than the PGUS. Random and conventional selections coincide in performance. It can be observed that as the required SU rate increases, improvement becomes less significant. As the transmit power becomes dominant, selection methods will no longer provide the benefit of reducing interference, since no matter which SU is chosen, the interference is overwhelming. To compare the proposed PGUS with the brute force user selection search, the simulation result for the BF US is also shown when $C = 3$. It can be seen that a complete search has slightly better performance when the required SU rate is low. can be clearly seen that with little performance sacrifice, the proposed PGUS sliding window selection algorithm can achieve good performance with much lower computational complexity.

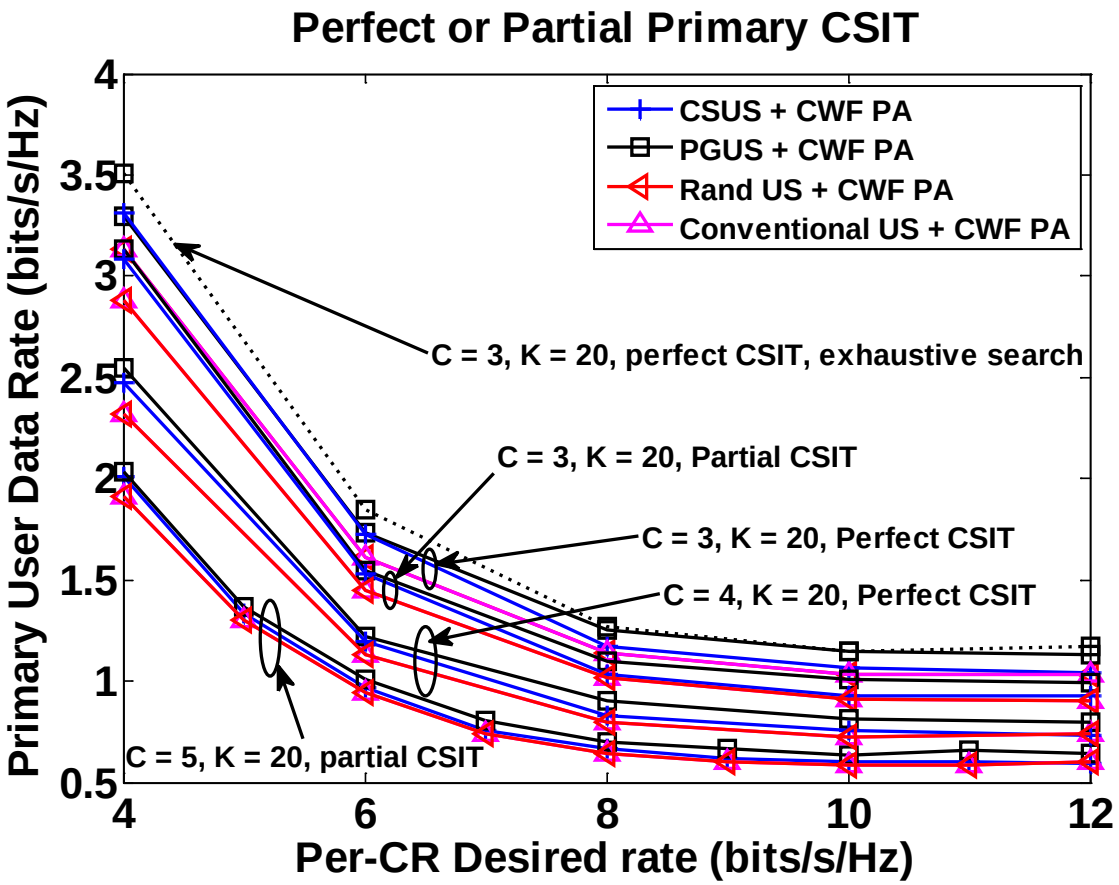

Figure 5.1: PU rate versus SU rate with perfect and partial primary CSIT $\mathbf{G}$

Figure 5.1 also shows the PU rate versus SU rate when the primary CSIT $\mathbf{G}$ is partially known at the CBS, for $C = 3, 5$ and $t = 15$. The primary interference channel $\mathbf{G}$ is modeled as $\mathbf{G} = \sqrt{\frac{K_{factor}}{K_{factor}+1}}\mathbf{M}_1 + \sqrt{\frac{1}{K_{factor}+1}}\mathbf{M}_2$, where $\mathbf{M}_1$ is the specular component that is known to the CBS, and $\mathbf{M}_2$ is the diffuse component that varies randomly across trials with Rician $K_{factor} = 8$ dB. Observe that the proposed PGUS and CSUS have better performance, e.g., 10% better at a SU rate of 4 bits/s/Hz/user, than the random and conventional user selections. However, as expected, the PU rate is degraded, in comparison to the perfect CSIT case.

Figure 5.2 displays the PU rate versus the SU rate when the primary CSIT $\mathbf{G}$ is not available at the CBS. Four user selection schemes were compared: CWF, FWF, BWF, and random selection employing the power allocation methods of CWF, FWF, BWF, and CWF,

respectively. Simulation conditions include SNR = 20 dB, $r_p = r = 3$, $t = 12$, $t_p = 4$, $K = 20$, and $C = 3, 4$. Observe that the proposed FWF and BWF greatly outperform the CWF, e.g., when the per-SU rate is 4 bits/s/Hz, the PU rate under the FWF is more than three times higher than that of CWF. The PU rates under FWF and BWF ultimately converge to CWF as the required SU rate increases, since FWF and BWF can no longer achieve R_k with lower transmission ranks. Finally, comparing Figure 5.1 with Figure 5.2, the results in Figure 5.2 show higher PU rates (e.g., three times at an SU rate of 4 bits/s/Hz/User) than those in Figure 5.1. In other words, the case of no CSIT with the proposed FWF or BWF shows better performance than the case of known CSIT with PGUS or CSUS. This is because FWF and BWF not only affect the selection result but also attempt to optimize the power allocation matrix $\mathbf{\Lambda}_k$ of selected SUs. In contrast, PGUS and CSUS, as shown in Figure 5.1 used conventional CWF for power allocation. This demonstrates that transmission rank optimization is highly beneficial even when primary CSIT is known. Note that in both cases, the CSIT between an SU transmitter and receiver is known to CBS; the difference is that the CBS has knowledge of interference channel $\mathbf{G}$ from the CBS to the PU receiver or not. Figure 5.2 also compares two hybrid schemes: CSUS with BWF power allocation and PGUS with BWF power allocation. This figure shows that when combined with BWF, CSUS and PGUS are much better than other curves with the same setup. This is because the hybrid schemes are under the condition of primary CSIT $\mathbf{G}$, which is known to the CBS.

Figure 5.3 shows that the PU rate as C varies when primary CSIT is completely unavailable. The SU desired rate was fixed at $R_k = 3$ bits/s/Hz and $C = 2, 4, 6, 8$. Again, the proposed BWF and FWF outperform the conventional CWF and random selection schemes for all C. The reason for the overlapping of BWF and FWF rates is that the SU target rate was set to a relatively low value, which could be achieved by using the same number of spatial dimensions on average. When the number of selected SUs increases, the PU rate decreases. This is intuitive since serving additional SUs generates extra interference from the CBS to the PU.

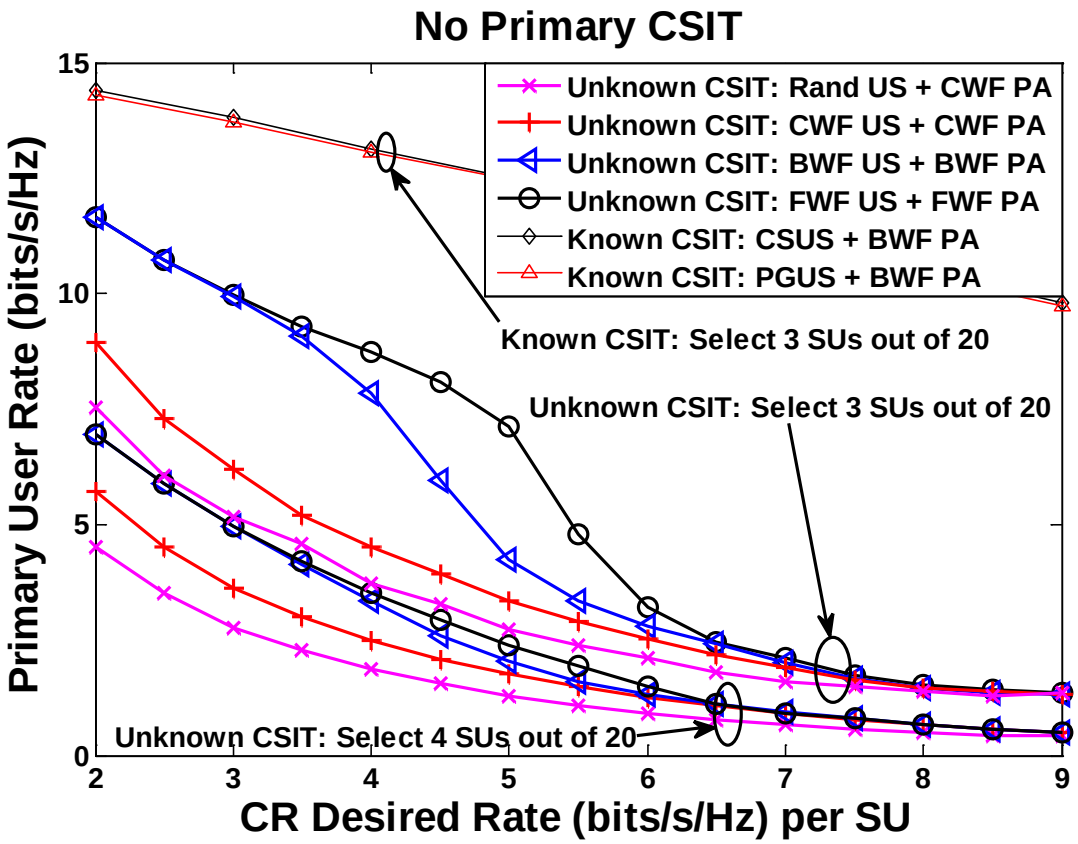

Figure 5.2: PU rate versus SU rate with no primary CSIT.

Figure 5.4 illustrates the maximum number of SUs supported on average for different PU IT constraints, assuming PU CSIT is perfectly known. The simulation condition includes SNR = 8 dB, $R_k = 4$ bits/s/Hz per SU, and $t = 15$. For each IT constraint, the maximum number of SUs supported is found by increasing C by one at a time until its IT exceeds the given IT constraint. The average number of supported SUs is calculated by taking 100 Monte Carlo iterations. It can be seen that PGUS can support a greater number of SUs under various IT constraints than a random selection. As the IT constraint increases, advantages of the PGUS become larger. Note that since $t = 15$, the maximum number of SUs supported without considering IT is 5, which is achieved by PGUS at an IT constraint of 20 dB. Random selection cannot do this.

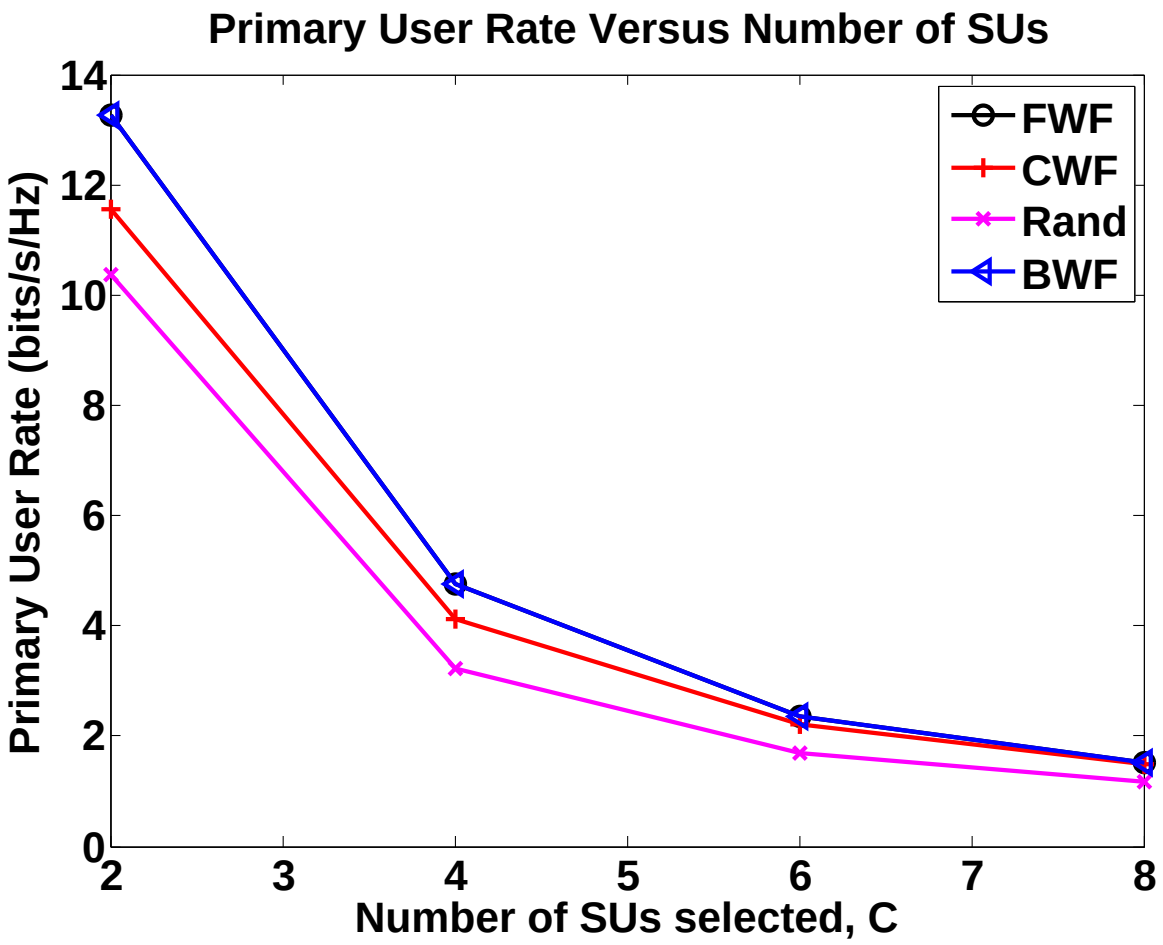

Figure 5.3: PU rate versus number of SUs with no primary CSIT, SU rate = 3 bits/s/Hz.

Table 5.1 summarizes the differences between the two cases of known and unknown CSIT $\mathbf{G}$ from the CBS to the PU RX at the CBS. User selection schemes and the corresponding power allocation methods are different for the two cases. Hence, the rank of $\mathbf{Q}_{CBS} = \sum_{j=1}^{C} \mathbf{Q}_j$ for the known CSIT case can be higher than that of the unknown CSIT case. Figure 5.5, which shows the $rank(\mathbf{Q}_{CBS})$ vs the per-SU data rate through simulation, verifies that the $rank(\mathbf{Q}_{CBS})$ for the CWF power allocation is higher than that of the BWF and FWF power allocation. It was proven in Proposition 1 in the work of Pei et al. [36] that the interference at the PU RX caused by the CBS gets lower as the rank of $\mathbf{Q}_{CBS}$ approaches one. Since the data rate of the PU decreases as the interference increases, a combination of FWF user selection + FWF power allocation has greater data rate than that of CSUS

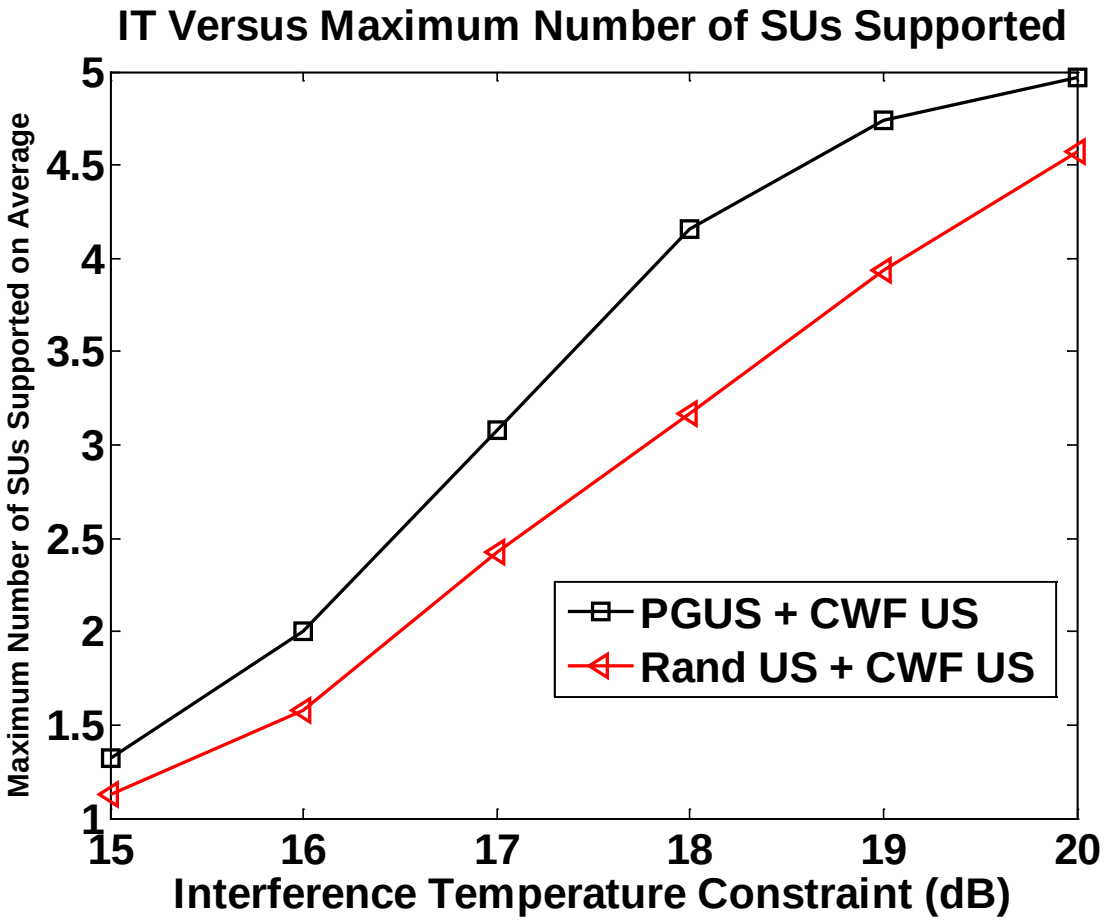

Figure 5.4: IT versus number of maximum SUs supported on average.

+ CWF PA. Similar conclusions can be made for the comparison of other combinations comparison.

More precisely, Figure 5.5 shows the ranks of transmitted covariance matrix $\mathbf{Q}_{CBS}$ of CBS TX averaged over, 1000 randomly generated channels $(\mathbf{F}, \mathbf{H}_j, \mathbf{G})$ for FWF US + FWF PA and CSUS + CWF PA. The proposed FWF US + FWF PA under even unknown CSIT can have lower ranks than the CSUS + CWF PA under known CSIT $\mathbf{G}$ because of in efficient conventional water-filling PA versus efficient proposed FWF PA.

When C SUs are selected out of K, there are $\binom{K}{C}$ possible combinations. Among these, there is at least one optimal combination and one worst combination. In an optimal combination, the channel matrices $\mathbf{H}_j$ of the selected C SUs are highly dissimilar to the

Table 5.1: Differences Between Two Cases: With and Without CSIT Matrix G

Difference	**With CSIT G**		**Without CSIT G**
User Selection Algorithm	CSUS (Algorithm 1), PGUS (Algorithm 2)		FWF, BWF (Algorithm 3)
Power Allocation Algorithm	CWF	BWF/FWF	FWF, BWF
Rank($\mathbf{Q}_{CBS}$), $\mathbf{Q}_{CBS} \triangleq$ Covariance Matrix of the CBS Transmitted Signal $= \sum_{j=1}^{C} \mathbf{Q}_j$	High to Full	Low to one	Low to One
Interference at PU RX $\propto$ Rank($\mathbf{Q}_{CBS}$) (Refer to [[36] Proposition 1])	High	Very Low	High

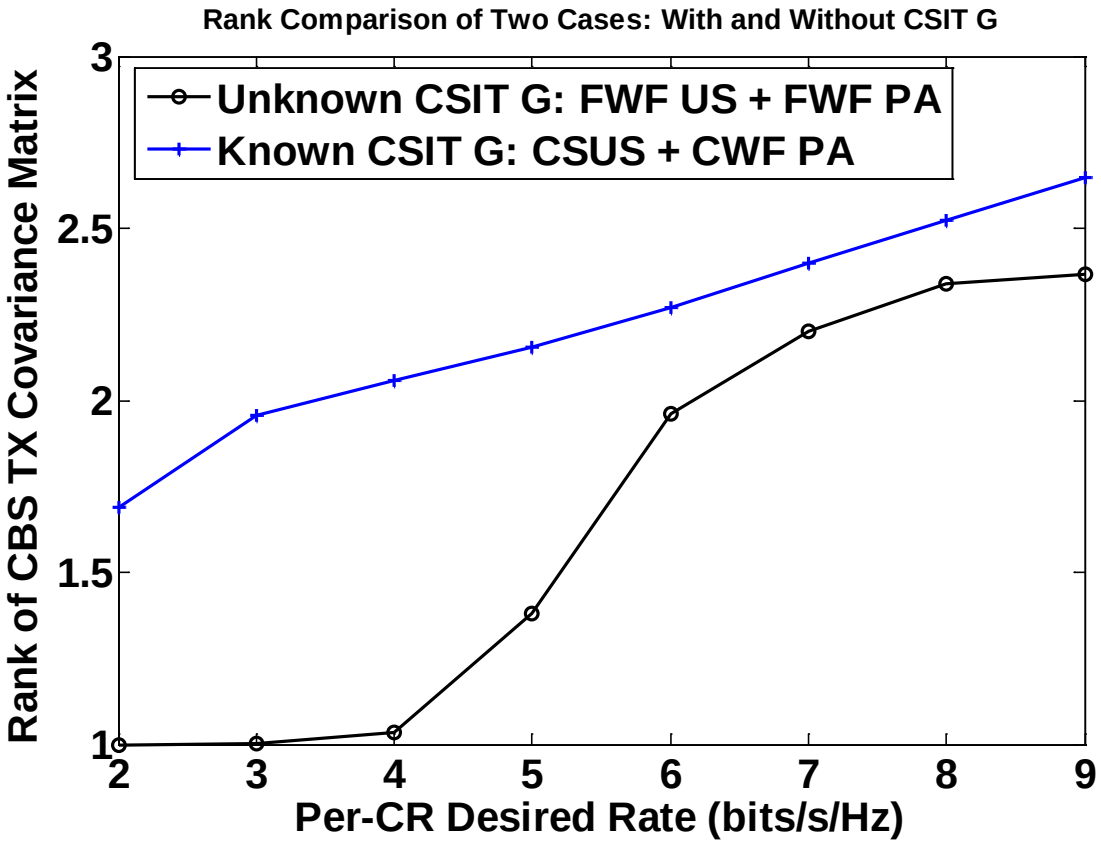

Figure 5.5: Rank Comparison of two cases: with and without CSIT **G**.

cross-channel interference matrix $\mathbf{G}$. Hence, interference from the CBS to the PU RX would be small, and the PU data rate can be high. The opposite is true in the worst combination where the SU channel matrices $\mathbf{H}_j$ are aligned with $\mathbf{G}$. Figure 5.6 shows the PU data rate versus the SU data rate similar to Figure 5.2 for the worst and best combinations when a set of channel matrices ($\mathbf{F}, \mathbf{H}_j$, and $\mathbf{G}$) are generated randomly and fixed, using Algorithm 3 (i.e., unknown CSIT $\mathbf{G}$), $j = 1, 2, ..., K(= 20)$ and $C = 3$. Here, an exhaustive search was used to find the best and worst combination cases. Using the proposed combination and PA Algorithm 3, it can be observed that the proposed algorithm performs close to the best case when the SU data rate is low and much better than the worst combination. Figure 5.6 also shows the best PU data rate versus SU data rate averaged over a set of 1,000 different channel matrices ($\mathbf{F}, \mathbf{H}_j$, and $\mathbf{G}$). Algorithms 1 and 2 also show similar trends.

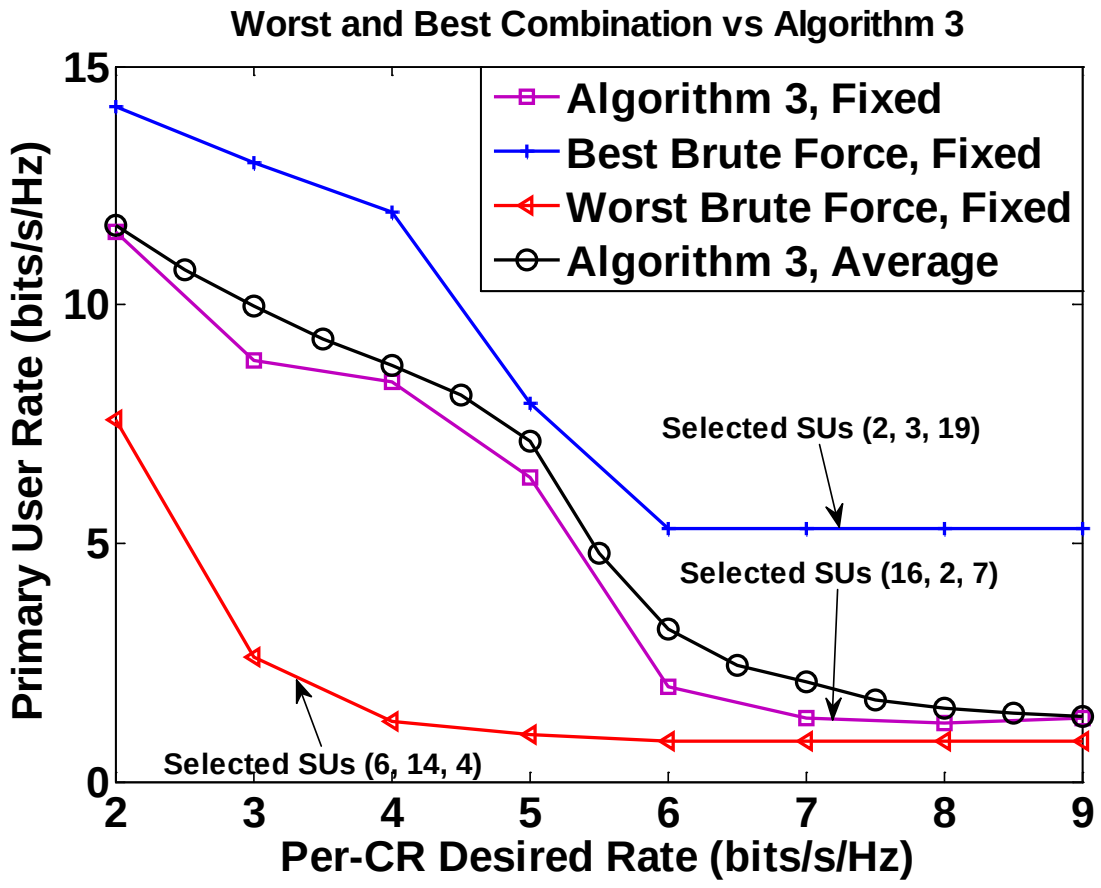

Figure 5.6: PU rate versus SU rate when the channel matrix $\mathbf{G}$ is unknown.

This section also shows the simulation results of improved QoS, C-UE sum rates, and D2D UE sum rates for cellular UE system that coexists with the D2D UE. In this part of the simulation, the conditions are $C = 15, M = 10, K = 25, Ne = Nc = Nd = 8$, $P_i = 8$ dB if $i \leq C$ and 6 dB otherwise, and the target data rate for C-UE varies from 20 to 24 bits/s/Hz. All D2D UE is assumed to allocate its power equally to all independent channel components.

Figure 5.7 shows the number of C-UEs meeting their rate target versus target rate $\bar{R}$ for two categories of resource sharing. Case 1 represents orthogonal resource sharing where C-UEs can not be assigned to $\mathcal{K}_d$, and case 2 indicates nonorthogonal resource sharing C-UEs can be assigned to all subchannels within $\mathcal{K}_d$. It can be observed that in case 2, almost twice as many C-UEs that are able to achieve their target data rates than case 1. This value decreases as the target data rate of C-UEs increases for both cases; performance of case 1 degrades to 7 C-UEs. As 15 additional subchannels are available to the 15 C-UEs in case 2, which means on average, 2 subchannels are allotted to one C-UE in the high target rate regime.

Figure 5.8 shows the D2D UEs sum rate versus C-UEs target data rate $\bar{R}_i$ with non-orthogonal resource sharing between CUEs and D2D UEs. The cost of accommodating more C-UEs at their target data rate is quantified by the 33% reduction in D2D UE sum rate compared to the orthogonal resource sharing approach. It can be observed that the D2D UEs sum rate is significantly higher when using FWF and BWF instead of classical MIMO waterfilling. This is because C-UEs create less interference to D2D UEs when using FWF and BWF. The assignment swapping step of the protocol provides additional benefit in terms of D2D UE interference mitigation due to transmit rank reduction of the C-UEs. It can be also seen that the D2D UEs sum rate expectedly decreases as the C-UE target data rate increases, due to the increase in the number of interfering spatial streams and transmit power from the C-UEs.

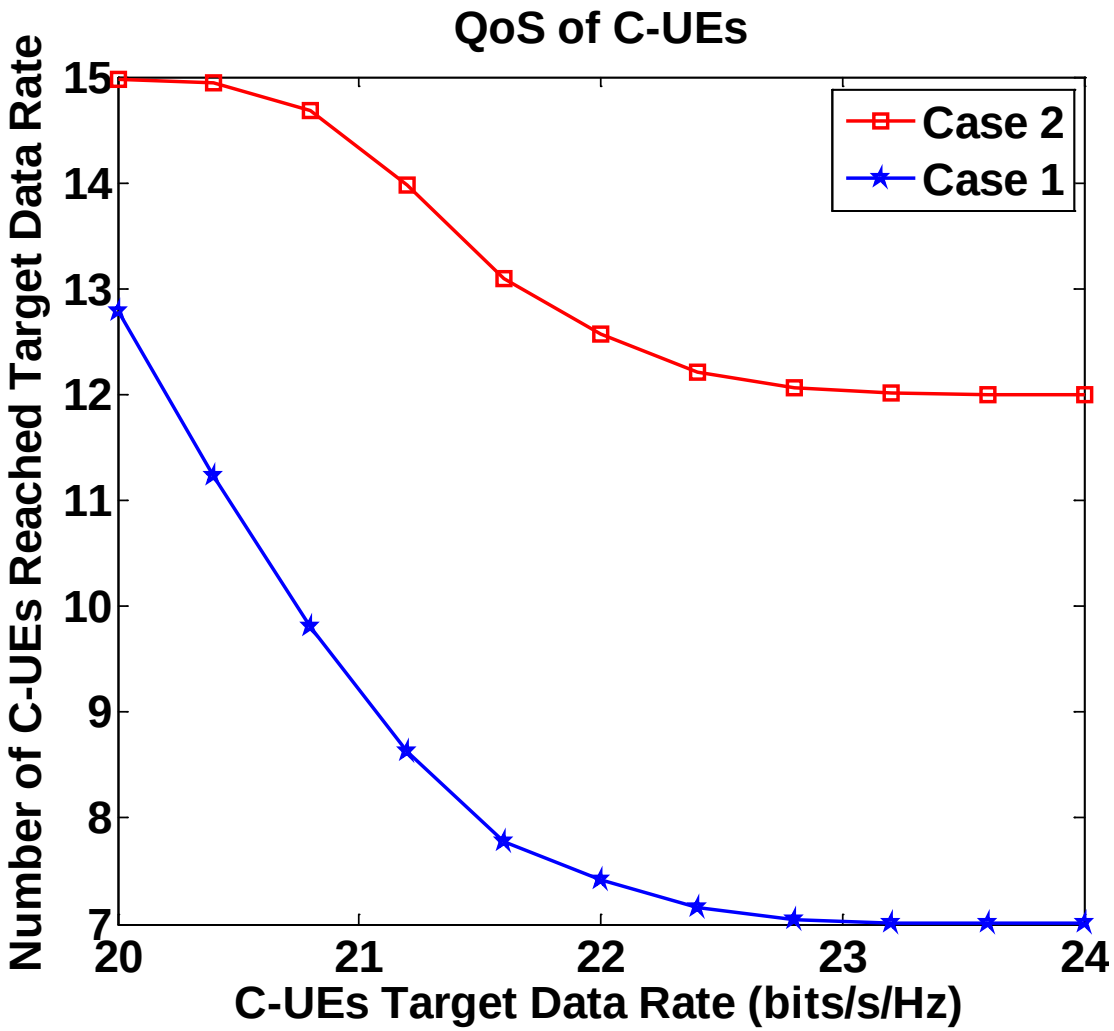

Figure 5.7: QoS of C-UE

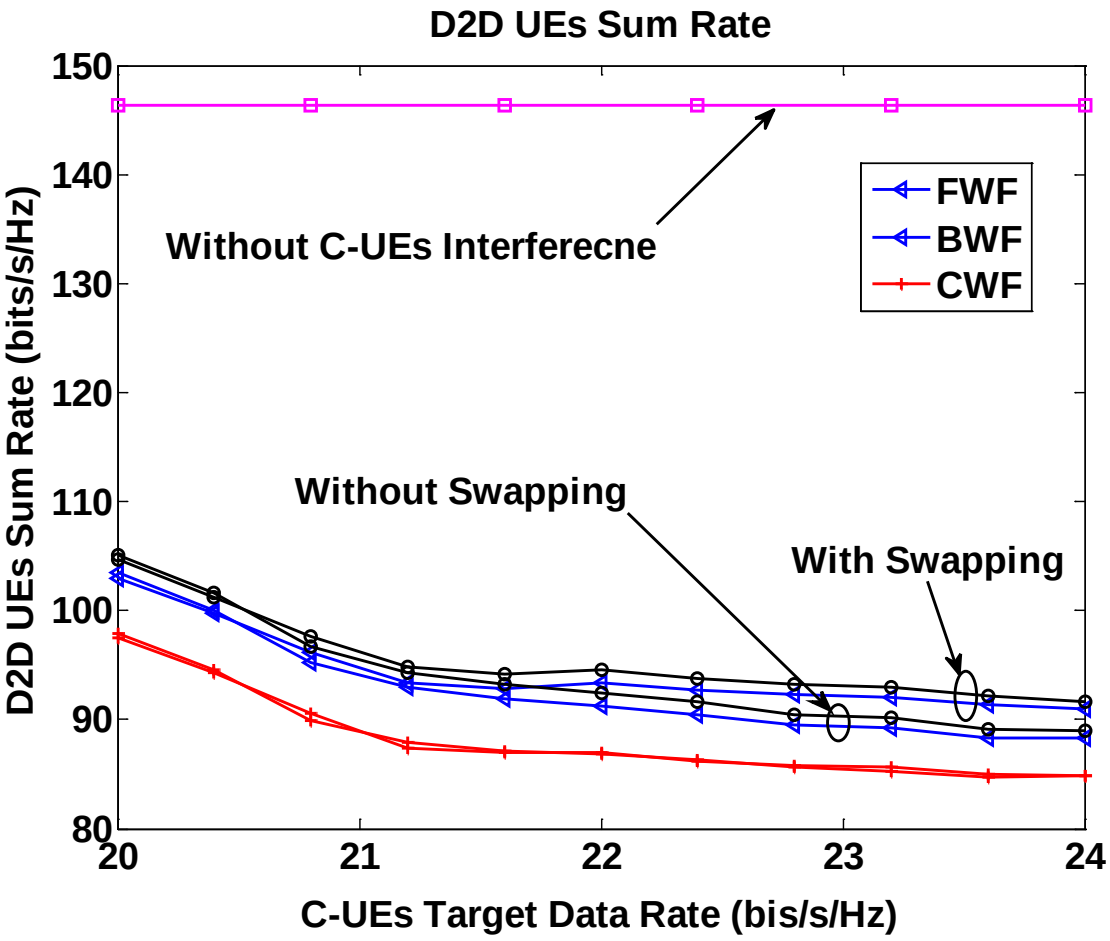

Figure 5.8: D2D UE rate when a subchannel is shared with a single C-UE, $N_c = N_d = 8$.

CHAPTER 6

CONCLUSION

Four new CR user selection schemes were presented for two scenarios, i.e., when primary CSIT is available and when it is not available. The proposed PGUS and CSUS for the perfect primary CSIT scenario exploits this channel knowledge either to apply best-effort interference mitigation or to adhere to hard IT constraints. For the scenario when primary CSIT is not available, only the best-effort interference mitigation is possible, and the SU selection schemes are designed based on either minimizing the transmission rank of SUs' channels or the rank-power product for a given SU data rate requirement. For future work, extensions to the interference channel scenario with multiple CBSs and PUs who use the common frequency bands are of interest.

A new solution for the coexistence of C-UE and D2D UE was also proposed. By assigning C-UE to $\mathcal{K}_d$, i.e., the set of subchannels assigned to D2D UEs, the QoS of C-UE can be increased significantly. Two new greedy power allocation water filling schemes were also proposed. These schemes reduce the interference that C-UE may cause to D2D UE. This can allow the D2D UEs to maintain their normal data transmission.

REFERENCES

LIST OF REFERENCES

[1] E. Hossain, D. Niyato, and Z. Han, *Dynamic Spectrum Access and Management in Cognitive Radio Networks*. Cambridge University Press, 2009.

[2] R. Zhang and Y. C. Liang, "Exploiting multi-antennas for opportunistic spectrum sharing in cognitive radio networks," *IEEE J. Sel. Topics Signal Process.*, vol. 2, pp. 88-102, Feb. 2008.

[3] A. Tajer, N. Prasad, and X. Wang, "Beamforming and rate allocation in MISO cognitive radio networks," *IEEE Trans. Signal Process.*, vol. 58, no. 1, pp. 362-377, Jan. 2010.

[4] A. Mukherjee and A. L. Swindlehurst, "Prescient precoding in heterogeneous DSA networks with both underlay and interweave MIMO cognitive radios," *IEEE Trans. Wireless Commun.*, vol. 12, no. 5, pp. 2252-2260, May 2013.

[5] L. B. Le and E. Hossain, "Resource allocation for spectrum underlay in cognitive wireless networks," *IEEE Trans. Wireless Commun.*, vol. 7, no. 12, pp. 5306-5315, Dec. 2008.

[6] I. Mitliagkas, N. D. Sidiropoulos, and A. Swami, "Joint power and admission control for ad-hoc and cognitive underlay networks: Convex approximation and distributed implementation," *IEEE Trans. Wireless Commun.*, vol. 10, no. 12, pp. 4110-4121, Dec. 2011.

[7] B. Zayen, A. Hayar, and G. E. Øien, "Resource allocation for cognitive radio networks with a beamforming user selection strategy," *Proc. of 43rd Asilomar Conf.*, 2009.

[8] K. Hamdi, W. Zhang, and K. B. Letaief, "Opportunistic spectrum sharing in cognitive MIMO wireless networks," *IEEE Trans. Wireless Commun.*, vol. 8, no. 8, pp. 4098-4111, Aug. 2009.

[9] H. Islam, Y. Chang Liang, and A. Hoang, "Joint power control and beamforming for cognitive radio networks," *IEEE Trans. Wireless Commun.*, vol. 7, no. 7, pp. 2415-2419, Jul. 2008.

[10] R. Imran, M. Odeh, N. Zorba, and C. Verikoukis, "Quality of experience for spatial cognitive systems within multiple antenna scenarios," *IEEE Trans. Wireless Commun.*, vol. 12, no. 8, pp. 4153-4163, Dec. 2013.

[11] E. Driouch and W. Ajib, "Downlink scheduling and resource allocation for cognitive radio MIMO networks," *IEEE Trans. Veh. Technol.*, vol. 62, no. 8, pp. 3875-3885, Oct. 2013.

[12] K. Doppler, M. Rinne, C. Wijting, C. B. Ribeiro, and K. Hugl, "Device-to-device communication as an underlay to LTE-Advanced networks," *IEEE commun. Mag.*, vol. 47, no. 12, pp. 42-49, Dec, 2009.

LIST OF REFERENCES (continued)

[13] 3GPP TR 22.803 V1.0.0, "Feasibility study for proximity services," `www.3gpp.org`, 2012.

[14] 3GPP TR 36.843 V12.0.1, "Study on LTE device to device proximity services; Radio aspects," `www.3gpp.org`, 2014.

[15] P. Janis, V. Koivunen, C. Ribeiro, J. Korhonen, K. Doppler, and K. Hugl, "Interference-aware resource allocation for device-to-device radio underlaying cellular networks," *Proc. of IEEE VTC Spring*, 2009.

[16] C.-H. Yu, K. Doppler, C. B. Ribeiro, and O. Tirkkonen, "Resource sharing optimization for device-to-device communication underlaying cellular networks," *IEEE Trans. Wireless Commun.*, vol. 10, no. 8, pp. 2752-2763, Aug. 2011.

[17] N. Naderializadeh and A. S. Avestimehr, "ITLinQ: A new approach for spectrum sharing in device-to-device communication systems," 2014, [Online]. Available: arXiv:1311.5527v3.

[18] X. Lin, J. Andrews, and A. Ghosh, "Spectrum sharing for device-to-device communication in cellular networks," [Online]. Available: arXiv:1305.4219.[cited May 13, 2014].

[19] Z. Zhou, M. Dong, K. Ota, J. Wu, and T. Sato, "Distributed interference-aware energy-efficient resource allocation for device-to-device communications underlaying cellular networks," 2014, [Online]. Available: arXiv:1405.1963v1.

[20] L. Lei, Z. Zhong, C. Lin, and X. Shen, "Operator controlled device-to-device communications in LTE-advanced networks," *IEEE Wireless Commun.*, vol. 19, no. 3, pp. 96-104, Jun. 2012.

[21] X. Lin, J. G. Andrews, A. Ghosh, and R. Ratasuk, "An overview of 3GPP device-to-device proximity services," *IEEE Commun. Mag.*, vol. 52, no. 4, pp. 40-48, Apr. 2014.

[22] G. Fodor, E. Dahlman, G. Mildh, S. Parkvall, N. Reider, G. Miklos, and Z. Turanyi, "Design aspects of network assisted device-to-device communications," *IEEE Trans. Commun.*, vol. 50, no. 3, pp. 170-177, Mar. 2012.

[23] A. Asadi, Q. Wang, and V. Mancuso, "A survey on device-to-device communication in cellular networks," *IEEE Commun. Surveys Tuts.*, to appear, 2014.

[24] D. Feng, L. Lu, Y. Yuan-Wu, G. Y. Li,G. Feng, and S. Li, "Device-to-device communications underlaying cellular networks," *IEEE Trans. Commun.*, vol. 61, no. 8, pp. 3541-3551, Aug. 2013.

LIST OF REFERENCES (continued)

[25] P. Phunchongharn, E. Hossain, and D. I. Kim, "Resource allocation for device-to-device communications underlaying LTE-advanced networks," *IEEE Wireless Commun.*, vol. 20, no. 4, pp. 91-100, Aug. 2013.

[26] D. Zhu, J. Wang, A. L. Swindlehurst, and C. Zhao, "Downlink resource reuse for device-to-device communications underlaying cellular networks," *IEEE Signal Process. Lett.*, vol. 21, no. 5, pp. 531-533, May 2014.

[27] D. H. Lee, K. W. Choi, W. S. Jeon, and D. G. Jeong, "Two-stage semi-distributed resource management for device-to-device communication in cellular networks," *IEEE Trans. Wireless Commun.*, vol. 13, no. 4, pp. 1908-1920, Apr. 2014.

[28] L. Wang and H. Wu, "Fast pairing of device-to-device link underlay for spectrum sharing with cellular users," *IEEE Commun. Lett.*, vol. 18, no. 10, pp. 1803-1806, Oct. 2014.

[29] C. Xu et al., "Efficiency resource allocation for device-to-device underlay communication systems: A reverse iterative combinatiorial auction based approach," *IEEE J. Sel. Areas Commun.*, vol. 31, no. 9, pp. 348358, Sept. 2013.

[30] A. Mukherjee and A. Hottinen, "Energy-efficient device-to-device MIMO underlay networks with interference constraints," *Proc. of ITG International Workshop on Smart Antennas*, Dresden, Germany, Mar. 2012.

[31] T. Yoo and A. Goldsmith, "On the optimality of multiantenna broadcast scheduling using zero-forcing beamforming," *IEEE J. Sel. Areas Commun.*, vol. 24, no. 3, pp. 528-541, Mar. 2006.

[32] S. Kaviani and W.A. Krzymień, "User selection for multiple-antenna broadcast channel with zero-forcing beamforming," in *Proc. IEEE GLOBECOM*, 2008.

[33] Z. Shen, J. G. Andrews, R. W. Heath, and B. L. Evans, "Low complexity user selection algorithms for multiuser MIMO systems with block diagonalization," *IEEE Trans. Signal Process.*, vol. 54, no. 9, pp. 3658-3663, Sep. 2006.

[34] R. D. Taranto, H. Yomo, P. Popovski, K. Nishimori, and R. Prasad, "Cognitive mesh network under interference from primary user," *Springer Wireless Personal Commun.*, spl. issue on Cognitive Radio Technologies, Feb. 2008.

[35] H. Yomo, P. Popovski, R. Prasad, K. Nishimori, Y. Takatori, and S. Kubota, "Interference exploitation for cognitive radios," *NTT Technical Review*, Oct. 2007.

[36] M. Pei, A. Mukherjee, A. L. Swindlehurst, and J. Wei, "Rank minimization designs for underlay MIMO cognitive radio networks with completely unknown primary CSI," in *Proc. IEEE GLOBECOM*, Anaheim, CA, Dec. 2012.

LIST OF REFERENCES (continued)

[37] B. Clerckx, H. Lee, Y.-J. Hong, and G. Kim, "A practical cooperative multicell MIMO-OFDMA network based on rank coordination," *IEEE Trans. Wireless Commun.*, vol. 12, no. 4, pp. 1481-1491, Apr. 2013.

[38] A. Mukherjee and A. L. Swindlehurst, "Modified waterfilling algorithms for multi-priority MIMO spatial multiplexing," *IEEE Wireless Commun. Lett.*, vol. 1, no. 2, pp. 89-92, Apr. 2012.

[39] Q. Spencer, A. L. Swindlehurst, and M. Haardt, "Zero-forcing methods for downlink spatial multiplexing in multi-user MIMO channels," *IEEE Trans. Signal Process.*, vol. 52, no. 2, pp. 461-471, Feb. 2004.

[40] H. Ding, J. Ge, and Z. Jiang, "Asymptotic performance analysis of amplify-and-forward with partial relay selection in Rician fading," *Electronics Lett.*, vol. 46, no. 3, 4th. Feb. 2010.

[41] T. Xu, J. Ge, and H. Ding, "An efficient distributed link selection scheme for AF-based cognitive selection relaying networks," *IEEE Commun. Lett.*, vol. 18, no. 2, Feb. 2014.

[42] P. Janis, V.Koivunen, C. Ribeiro, J. Korhonen, K. Doppler, and K. Hugl, "Interference-aware resource allocation for device-to-device radio underlaying cellular networks," in *Proc. of IEEE VTC,* Spring, 2009.